

SCIENTIFIC REPORTS



OPEN

Rate of entropy model for irreversible processes in living systems

R. Zivieri^{1,2}, N. Pacini³, G. Finocchio² & M. Carpentieri⁴

In living systems, it is crucial to study the exchange of entropy that plays a fundamental role in the understanding of irreversible chemical reactions. However, there are not yet works able to describe in a systematic way the rate of entropy production associated to irreversible processes. Hence, here we develop a theoretical model to compute the rate of entropy in the minimum living system. In particular, we apply the model to the most interesting and relevant case of metabolic network, the glucose catabolism in normal and cancer cells. We show, (i) the rate of internal entropy is mainly due to irreversible chemical reactions, and (ii) the rate of external entropy is mostly correlated to the heat flow towards the intercellular environment. The future applications of our model could be of fundamental importance for a more complete understanding of self-renewal and physiopatologic processes and could potentially be a support for cancer detection.

The irreversible processes in living systems are fundamental for determining the autopoietic life development and lead to entropy production in living systems^{1–3}. Examples of irreversible chemical reactions that represent basic processes both for prebiotic life and for life development and maintenance are sodium/potassium pump, β -oxidation of fatty acids, protein catabolic process, glucose catabolism, etc. The full understanding of the non-equilibrium thermodynamics of irreversible reactions is important for the origin and the maintenance of life^{4,5}. Very interestingly, while mechanical phenomena are invariant under time-reversal symmetry, thermodynamic ones introduce an arrow of time breaking this symmetry. This behaviour is naturally linked to the concept of entropy⁶ that, according to its first definition by Clausius and Boltzmann^{7,8}, describes the thermodynamics of catabolic processes.

Recent works have shown that there is a link between the irreversible processes in the metabolic network, such as glucose catabolism, and epigenetic and gene network^{9–13}, and that the entropy definition introduced by Clausius and Boltzmann^{7,8} is equivalent to Shannon information entropy^{14–19}. Since the 20s^{20,21}, it is known that almost all cancer cells show a deep alteration of their metabolic networks with a marked shift towards the lactic acid fermentation or aerobic glycolysis at the expense of oxidative phosphorylation (OXPHO). Interestingly, the relation between the glucose catabolism and the gene and epigenetic network strengthens during the cancer development^{22–28}, likewise there has been a wide use of the intensity of aerobic glycolysis in diagnostics with correlations to cancer prognosis^{29–31}.

Although it is well-known the crucial role played by irreversible reactions in living systems, a self-consistent description of the calculation of the entropy exchanges between the cell and the environment is missing. This is because the quantitative description of cell thermodynamics is still incomplete. Furthermore, the important quantitative aspects related to the time behaviour of entropy have not been taken into account. Indeed, it has emphasized the exergy concept regardless of the ATP yield and of coupling between exo- and endo-ergonic reactions^{32,33}. In other words, the concept of rate of entropy is different from the concepts of finite variations of entropy and Gibbs free energy between reactants and products. Moreover, some *in vitro* experiments and biophysical theoretical investigations have proved that the heat flow is not only the simple effect of degradation of

¹Department of Physics and Earth Sciences and Consorzio Nazionale Interuniversitario per le Scienze Fisiche della Materia, Unit of Ferrara, University of Ferrara, via G. Saragat 1, Ferrara, I-44122, Italy. ²Department of Mathematical and Computer Sciences, Physical Sciences and Earth Sciences, University of Messina, V.le F. D'Alcontres, 31, 98166, Messina, Italy. ³Department of General Surgery and Senology, University Hospital Company, Policlinico Vittorio Emanuele, via S. Citelli 6, 95124, Catania, Italy. ⁴Department of Electrical and Information Engineering, Politecnico di Bari, via E. Orabona 4, Bari, I-70125, Italy. Correspondence and requests for materials should be addressed to R.Z. (email: roberto.zivieri@unife.it)

energy but plays also an important role in the ionic transport and in the interactions among biomolecules such as DNA, proteins and so on^{34–36}.

Here, we formulate a model relying on the Clausius definition of entropy and on Prigogine's approach able to give a full thermodynamic description of the rate of entropy density production associated to irreversible chemical processes in living systems. This model considers: i) the time dependence of the entropy exchanges in the cell and out of it, and ii) the effect of the cell size on the rate of entropy density production. We apply the model to the glucose catabolism in a typical human tissue represented by breast cells. The choice of glucose catabolism is essentially twofold. First, several recent works have shown its important role for the different pathways driving cancer development^{37–39}. Second, the glucose catabolism is, among the irreversible reactions occurring in cells, the one having the highest frequency of occurrence and the largest entropy production⁴⁰. The key result of our work on glucose catabolism is that the diffusion of chemical species gives the largest contribution to the rate of internal entropy density both in normal and cancer cells, while the rate of external entropy density, mainly due to heat diffusion, has an enhancement in cancer cells. Although most of cancer therapy is mainly pharmacological, a wider knowledge of the physical processes like, for example, the observation of temperature differences between the intracellular and the intercellular environment is important for developing new prospects in cancer detection^{41–43}. This latter aspect is widely coherent with the experimental trials and clinical data, and could open new perspectives on the hyperthermia cancer therapy^{44,45}.

Model for the calculation of the rate of entropy in living systems. We have studied the cell as an open thermodynamic system in local equilibrium. Hence, starting from Prigogine's approach⁴⁶ combined with diffusion equations valid for heat and mass transport, we have computed the rate of entropy density production $r = ds/dt$ for a cell with s entropy density and t time (see Methods). The exchange of entropy occurs at two different levels, in the cell interior and with the intercellular environment, hence $r = r_i + r_e$ where $r_i = ds_i/dt$ is the rate of internal entropy density production (RIEDP) where the subscript "i" denotes internal and $r_e = ds_e/dt$ is the rate of external entropy density production (REEDP) where the subscript "e" denotes external. To calculate r_i we have made the following main assumptions:

- (i) Cells are assumed of cubic shape having volume $V_{\text{cell}} = L^3$ with L the side of the average cube;
- (ii) Flows are along a preferential direction (1D approximation) (x direction here);
- (iii) Irreversible processes start in the centre of the cytoplasm region, namely for $x = L/2$;
- (iv) Cross-effects in determining either the heat flow or the mass flow are absent;
- (v) The volume of the cell nucleus is negligible.

The model is applicable to any kind of chemical reaction involved in the metabolic cellular activity of living systems.

Assumption (i) allows the study of cells of various shapes (e.g. spherical, cylindrical, elliptical and so on) represented as cubes having volumes equivalent to those of the specific shape studied. In particular, assumption (i) applies to several epithelium tissues like, for example, the breast epithelium and the exocrine glands epithelium whose shape is columnar⁴⁷. As cellular processes occur prevalently along a preferential direction⁴⁸, typically assumption (ii) is valid in real systems. Assumption (iii) is supported by the fact that mitochondria, where most of the catabolic processes in normal and cancer cells occur (e.g. Krebs cycle, β -oxidation and part of protein catabolism), are approximately placed in the perinuclear region⁴⁹. Moreover, in cancer cells also lactic acid fermentation takes place in the mitochondrial region. However, note that in some cases a few catabolic reactions like, for instance chemotaxis, occur in cell peripheral zones. In these specific cases, it would be enough to make a translation of the origin of $L/2$ to the cell border. Assumption (iv) is consistent in the presence of polarization effects occurring in cells^{48,50}. Assumption (v) is reasonable in most of the cells being the volume of the nucleus much smaller than V_{cell} . By taking into account all the above assumptions, we have computed $r_i(x, t) = r_{iQ}(x, t) + r_{iD}(x, t) + r_{ir}(x, t)$ where $r_{iQ}(x, t)$ is due to heat flow with the subscript "Q" labelling heat, $r_{iD}(x, t)$ is caused by molecules diffusion with the subscript "D" standing for diffusion and $r_{ir}(x, t)$, with the subscript "r" indicating reactions, is directly related to irreversible chemical reactions. All terms are products between thermodynamic forces and flows generated by them. In explicit form, for any irreversible reactions, the contribution due to heat flow $r_{iQ}(x, t)$ is given by

$$r_{iQ}(x, t) = \alpha \frac{\left[\sum_{n=1}^{\infty} \left(\cos \left[(2n-1) \frac{\pi}{L} x \right] e^{-\kappa(2n-1)^2 \frac{\pi^2}{L^2} t} \right)^2 \right]}{[T(x, t)]^2} e^{-\frac{t}{\tau}} \quad (1)$$

Here, $\alpha = 16pK \frac{T_0^2}{L^2}$ with p the weight associated to the specific chemical reaction evaluated as a function of the occurrence frequency of the reaction, K is the thermal conductivity, κ is the thermal diffusivity and τ is a typical cell decay time. The term $T(x, t) = \frac{4T_0}{\pi} \sum_{n=1}^{\infty} \left(\sin \left[(2n-1) \frac{\pi}{L} x \right] / (2n-1) e^{-\kappa(2n-1)^2 \frac{\pi^2}{L^2} t} \right)$ is the temperature distribution (see Supplementary information, Section 2, equation (S3) and equation (S5)) showing that the temperature inside the cell has a weak spatial dependence coherently with the data obtained by means of fluorescent technique⁴³. The cosine series at the numerator results both from the calculation of the thermodynamic force calculated as the gradient of the inverse of the temperature distribution and the heat flow proportional to the spatial derivative of $T(x, t)$ (see Supplementary information, Section 2, equation (S6) and equation (S7), respectively).

Instead, for every irreversible process, $r_{iD}(x, t)$ takes the form

$$r_{iD}(x, t) = \beta \frac{(x - L/2)e^{-\frac{x}{L}}}{t^{3/2}} \left(\sum_{k=1}^N \left(u_k \frac{N_{mk}}{4\sqrt{D_k}} e^{-\frac{(x-L/2)^2}{4D_k t}} \right) \right) \left(\frac{\sum_{n=1}^{\infty} \left(\cos \left[(2n-1) \frac{\pi x}{L} \right] e^{-\kappa(2n-1)^2 \frac{\pi^2}{L^2} t} \right) e^{-|x-L/2|/L}}{[T(x, t)]^2} \right) \quad (2)$$

Here, $\beta = \frac{1}{\pi} \frac{1}{V_{\text{cell}}} T_0$, N is the number of chemical species involved in the reaction and $\mu_k(x, t) = u_k e^{-|x-L/2|/L+t/\tau}$ is the k^{th} chemical potential with u_k the partial molar energy, D_k is the corresponding mass diffusion coefficient and N_{mk} is the number of moles of the k^{th} chemical species. It is $e^{-(x-L/2)/L} (e^{-(L/2-x)/L})$ for $0 \leq x \leq L/2$ ($L/2 \leq x \leq L$). The cosine series at the numerator results from the thermodynamic force evaluated as the gradient of the ratio between the chemical potential and the temperature distribution, while the Gaussian distribution comes from the diffusion flow proportional to the derivative of the number of moles per unit volume (see Supplementary information, Section 2, equation (S11) and equation (S15), respectively).

Finally, $r_{ir}(x, t)$ is

$$r_{ir}(x, t) = -\gamma \frac{1}{V_{\text{cell}}^{p+q}} \frac{k_{\text{kin}} \left(\sum_{k=1}^N \nu_k u_k e^{-(x-L/2)/L+t/\tau} \right) N_{mA \text{ reag}}^p N_{mB \text{ reag}}^q}{[T(x, t)]^2} \quad (3)$$

where, $\gamma = \frac{4}{\pi} T_0$, k_{kin} is the pathway kinetic constant of the given irreversible process with “kin” standing for kinetic, ν_k are stoichiometric coefficients, $\mu_k(x, t) = u_k e^{-|x-L/2|/L+t/\tau}$ is the chemical potential of the k^{th} species. Here $p=0, 1, 2$, $q=0, 1, 2$ and $p+q=1, 2$ for first- and second-order irreversible chemical reactions, respectively and $\frac{N_{mA \text{ reag}}}{V_{\text{cell}}}$ ($\frac{N_{mB \text{ reag}}}{V_{\text{cell}}}$) is the molar concentration of reagent A (B) taking the volume of the solution equal to V_{cell} . The dependence on the chemical potential and on the molar concentrations at the numerator results from the definition of affinity and of the velocity of the given reaction (see Supplementary information, Section 2, equation (S20), equation (S21) and equation (S22), respectively). For the detailed derivation of equations (1–3), see Supplementary Information, Section 2.

We now discuss $r_e(x, t)$ calculated by taking into account assumptions (i), (ii) and (v). We express $r_e(x, t) = r_{eQ}(x, t) + r_{e \text{ exch}}(x, t)$, where $r_{eQ}(x, t)$ is the contribution due to heat released by the cell in the intercellular environment, while $r_{e \text{ exch}}(x, t)$, with “exch” standing for exchanges, is the one related to exchanges of matter with the intercellular environment.

The derivation of $r_{eQ}(x, t)$ lies on simple thermodynamic considerations. Specifically, we have used the first principle of thermodynamics for the expression of the heat released, the solution of heat equation in the intercellular environment (see Supplementary information, Section 3 equation (S29)) and exploiting the analogy of the behaviour of the cellular system mainly composed by water with that of an ideal gas. As in the case of a monoatomic gas, we derive the cell internal energy starting from its partition function that has a direct thermodynamic relation with the internal energy. It turns out that $r_{eQ}(x, t)$ reads

$$r_{eQ}(x, t) \simeq \delta \frac{N_{mpr} (x - L)^2}{\kappa t^2} \quad (4)$$

Here, $\delta = \frac{1}{V_{\text{cell}}} \frac{3}{8} k_B N_A$ with k_B the Boltzmann constant, N_A the Avogadro number and N_{mpr} is the number of moles of the products in every irreversible process.

Instead, $r_{e \text{ exch}}$ is

$$r_{e \text{ exch}}(x, t) = -\eta \frac{1}{t^2} e^{-\frac{(x-L)^2}{4\kappa t}} \sum_{k=1}^{N_{pr}} u_k e^{-|x-L/2|/L+t/\tau} \frac{d_e N_{mk}}{d\tau_1} \quad (5)$$

Here, $\eta = \frac{1}{V_{\text{cell}}} \frac{1}{x_0} \frac{(4\pi\kappa)^{\frac{1}{2}}}{T_0}$, where x_0 is a characteristic length of the order of the size of the normal cell, T_0 is the maximum intercellular temperature, $d\tau_1$ is a characteristic time of the order of the inverse of k_{kin} , N_{pr} is the number of products of the irreversible chemical process with “pr” indicating products and $d_e N_{mk}$ is the variation of the number of moles of the products of the irreversible reaction. To derive equation (5) we have substituted the intercellular temperature distribution determined by solving the heat equation in the intercellular environment with no boundary conditions and the expression of the chemical potential. For the detailed calculations leading to equations (4) and (5), respectively see Supplementary Information, Section 3 for the detailed.

As expected, equations (1)–(5) do not fulfil the time-reversal symmetry ($r(x, t) = r(x, -t)$) and this is an elegant demonstration of the irreversible nature of spontaneous processes occurring in living systems. Finally, note that the model developed for a single cell can be extended to a tissue by generalizing equations (1)–(5) to the number of cells composing it and by considering their mutual interactions but this is outside the scope of this work.

Application of the rate of entropy model to glucose catabolism in normal and cancer breast cells. We have applied the general model, described in the previous section, to glucose catabolism in a typical epithelial breast tissue. In a cell, the glucose catabolism is an essential step in the production of ATP for energy purposes. In general, in differentiated cells there is the production of about 80–90% of the ATP through OXPHOs,

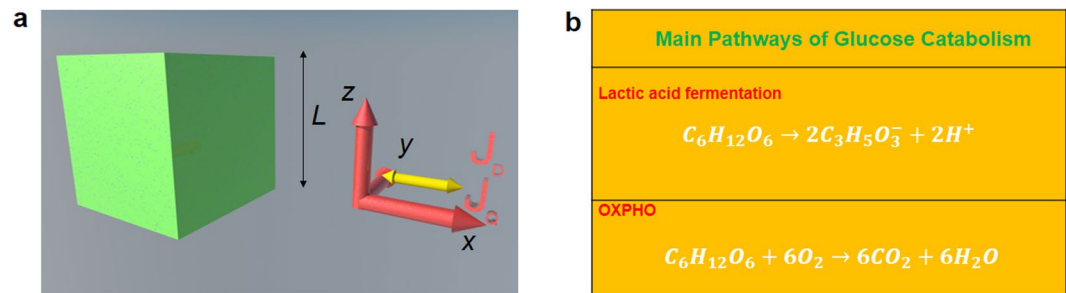


Figure 1. Cell representation and balancing of glucose catabolism. **(a)** Sketch of the cubic cell according to the cyto-morphological features of the epithelial tissue chosen as the reference tissue in our theoretical model. **(b)** Schematics of main pathways of glucose catabolism. The internal heat flow and the mass diffusion flow start in the cytoplasm region for $x = L/2$ and are along $+x$ and $-x$ directions as shown by the yellow arrows.

while in undifferentiated cells or cancer cells, where there is a prevalence of lactic acid fermentation, this ratio can considerably change and sometimes it can even invert. In the same interval of time the major rapidity of the fermentation process produces a high amount of ATP, as long as a high uptake of glucose and a high expression and activity of lactic acid dehydrogenase, conditions that are present in the predominantly fermentative cellular systems. In addition, there is a major number of processed molecules through the fermentative way in order to maintain a sufficient stock of ATP. In normal cells, the glucose catabolism is 80% through OXPHOs and 20% through lactic acid fermentation, while in cancer cells 90% occurs through lactic acid fermentation and 10% through OXPHOs^{20, 21}.

We show the representative cell (either normal or cancer) in the form of a cubic cell of average side L and the glucose catabolism process in Fig. 1 where J_Q is the internal heat flow and J_D is the internal diffusion flow.

In the numerical calculations, we have taken the typical sizes of epithelial cells of human breast tissue (normal or cancer). Specifically, we have employed an average size $L = 10 \mu\text{m}$ for the normal cell and $L = 20 \mu\text{m}$ for the cancer cell⁵¹. Moreover, the membrane between the cell and the intercellular environment is of the order of a few Angstroms and it is much smaller than the cell size so that it can be neglected. In addition, for the same tissue we have taken an average size of the intercellular space about $0.2\text{--}0.3 \mu\text{m}$ between two adjacent normal cells and about $1.5 \mu\text{m}$ between two cancer cells⁵². Within the 1D model employed the flows and the thermodynamic forces generating the flows occur along the x direction in the cytoplasm and on both sides. Indeed, according to assumption iii), we have considered that all processes originate in the centre of the cell at $x = L/2$ for values of y and z coordinates corresponding to cytoplasm region.

We distinguish between two kinds of reactions. The first one refers to the cell respiration process involving the catabolism of glucose ($\text{C}_6\text{H}_{12}\text{O}_6$) via the oxygen molecule (O_2) and consists of: (a) glycolysis (b) Krebs cycle and (c) oxidative phosphorylation. The general balancing of all reactions is summarized in the simple form $\text{C}_6\text{H}_{12}\text{O}_6 + 6\text{O}_2 \rightarrow 6\text{CO}_2 + 6\text{H}_2\text{O}$ leading to the formation of carbon dioxide (CO_2) and water (H_2O). The second process is the lactic acid fermentation process with no Krebs cycle and oxidative phosphorylation. The corresponding reaction leads to the formation of lactic acid ions ($\text{C}_3\text{H}_5\text{O}_3^-$) and is summarized in the simple form $\text{C}_6\text{H}_{12}\text{O}_6 \rightarrow 2\text{C}_3\text{H}_5\text{O}_3^- + 2\text{H}^+$. For our purposes, we have not considered the NAD^+/NADH and purine nucleotides such as $\text{ATP}/\text{ADP}/\text{AMP}$ ⁵³ because their concentrations vary within small ranges and do not affect the calculation of the RIEDP and REEDP. Furthermore, the oxide/reduction reactions of NAD^+/NADH are reversible and the reactions leading to ATP synthesis molecule are not spontaneous and processes irreversible^{54, 55}. For the sake of simplicity, note that here we describe the stoichiometric balancing of the above reactions by considering one mole of glucose even though during the glucose catabolism the range of glucose concentration in a single cell is between pico- and micromoles.

Results

Numerical calculation of the rate of internal entropy density production for breast cells.

Figure 2 shows the RIEDP calculated for a normal and cancer breast cell as a function of the spatial coordinate and time⁵⁶ obtained by using the chemical potentials and diffusion coefficients in Tab.1. The use of the chemical potential at standard conditions shown in Table 1 in the numerical calculations is justified by the fact that, within the ideal gas description of a cell, the temperature dependent chemical potential $\mu(T)$ is very close to the μ at standard conditions from the Gibbs-Duhem relation being the pressure inside a cell close to the atmospheric pressure.

We have chosen the time interval of $1000 \mu\text{s}$ because it is a typical internal time⁵⁷ for most biological processes. r_{iQ} was calculated using equation (1) taking $K = 0.600 \text{ J}/(\text{m s K})$, $\kappa_{\text{H}_2\text{O}} = 0.143 \times 10^{-6} \text{ m}^2/\text{s}$, the thermal diffusivity in water and $p = 0.85$ (0.90) for normal (cancer) cells^{21, 38}. r_{iD} was calculated according to equation (2), while $r_{i\tau}$ was calculated according to equation (3) applied to glucose catabolism (see Supplementary Information, Section 2, equations (S17) and (S26), respectively for more details). In addition, $N_{\text{resp}} = 4$ ($N_{\text{ferm}} = 3$) is the number of chemical species involved in the respiration (fermentation) process, $w_{\text{resp}} = 0.8$ ($w_{\text{ferm}} = 0.2$) with “resp” (“ferm”) labelling respiration (fermentation) are the corresponding weights of the respiration (fermentation) processes for a normal cell and $w_{\text{resp}} = 0.1$ ($w_{\text{ferm}} = 0.9$) for a cancer cell^{37–39}. We have also taken the pathway kinetic constants

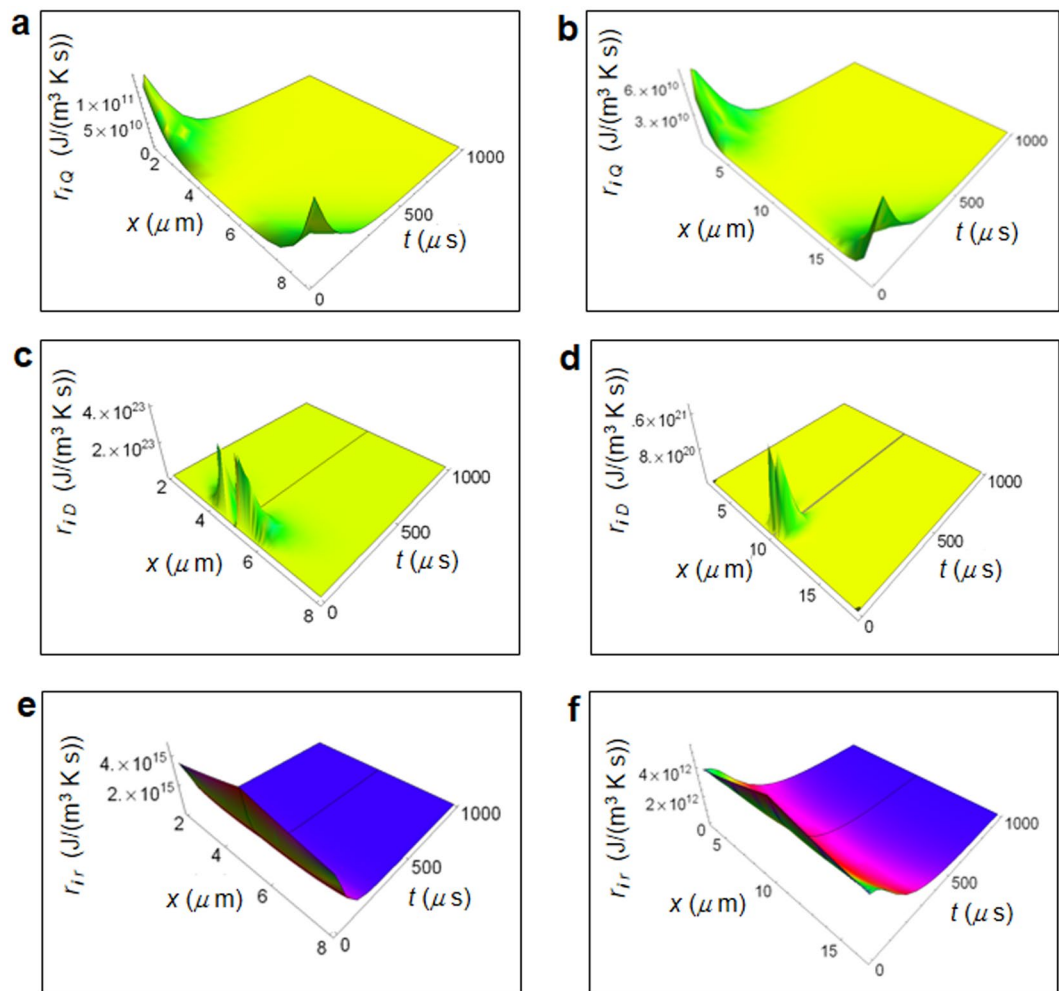


Figure 2. Calculated RIEDP during glucose catabolism for a breast cell. **(a)** RIEDP associated to heat flow for a normal cell. **(b)** RIEDP associated to heat flow for a cancer cell. **(c)** RIEDP related to matter diffusion for a normal cell. **(d)** RIEDP related to matter diffusion for a cancer cell. **(e)** RIEDP due to irreversible reactions for a normal cell. **(f)** RIEDP due to irreversible reactions for a cancer cell.

Chemical species	Chemical potential μ (kJ/mole) $T=298\text{ K}, p=1\text{ atm}$	Diffusion coefficient D in H_2O (m^2/s) $T=298\text{ K}, p=1\text{ atm}$
$\text{C}_6\text{H}_{12}\text{O}_6$	-917.44	6.73×10^{-10}
O_2	16.44	21.00×10^{-10}
CO_2	-385.99	19.20×10^{-10}
H_2O	-237.18	21.00×10^{-10}
Lactate ion $\text{C}_3\text{H}_3\text{O}_3^-$	-516.72	9.00×10^{-10}
H^+ aqueous solution	0	45.00×10^{-10}

Table 1. Chemical potentials and diffusion coefficients for the chemical species involved in glucose catabolism for cell respiration and lactic acid fermentation. The data are from G. Job and R. R uffler, *Physikalische Chemie*, Vieweg + Teubner Verlag Springer (2011).

$k_{\text{kin}}^{\text{resp}} = 10^{-4}/\text{s}$ and $k_{\text{kin}}^{\text{ferm}} = 10^{-5}/\text{s}$ and both processes, in general, are first-order chemical reactions⁵⁷. In addition, we have used $\tau = 10^{-4}\text{ s}$ as typical cell decay time and $N_m \text{C}_6\text{H}_{12}\text{O}_6 = 1$ for both respiration and fermentation processes.

r_{iQ} shown in Fig. 2a and b has a strong variation going towards cell borders and quickly decreases with time. r_{iD} depicted in Fig. 3c and d exhibits a significant magnitude close to the centre of the cell and strongly decreases towards the border and with increasing time. r_{ir} displayed in Fig. 2e and f is maximum close to the centre of the cell, slightly reduces the amplitude towards the cell border and strongly decreases with increasing time especially

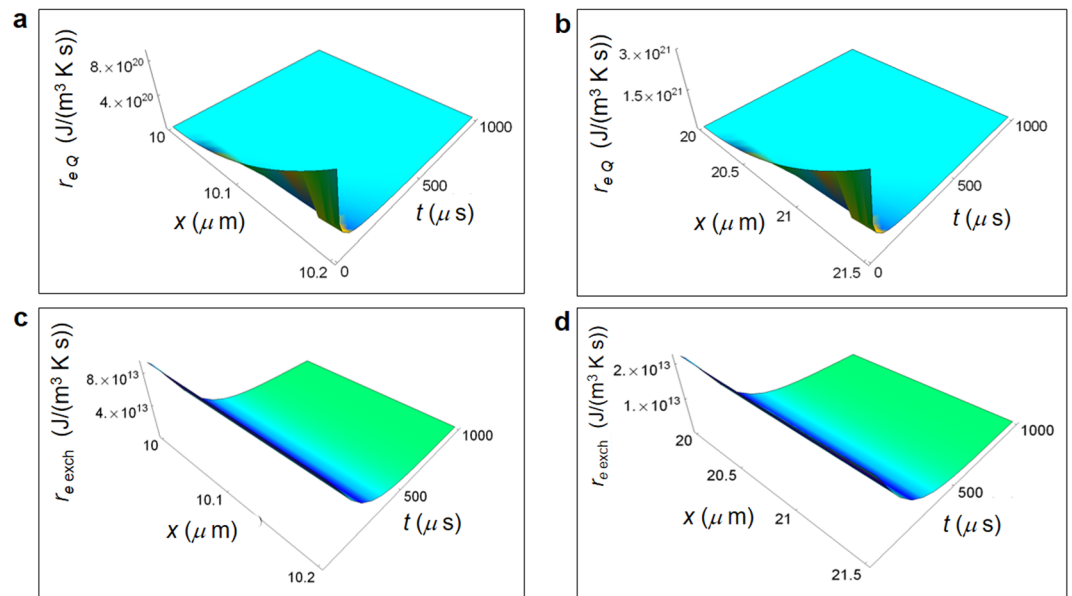


Figure 3. Calculated REEDP during glucose catabolism for a breast cell. **(a)** REEDP associated to heat flow for a normal cell as a function of the spatial and time coordinates. **(b)** REEDP associated to heat flow for a cancer cell. **(c)** REEDP due to exchange of matter for a normal cell. **(d)** REEDP due to exchange of matter for a cancer cell.

in a normal cell. Both r_{iD} and r_{ir} are much greater than r_{iQ} and are about two order of magnitude greater in a normal cell with respect to a cancer cell.

Numerical calculation of the rate of external entropy density production for breast cells.

Figure 3 displays calculated r_{eQ} and $r_{e\text{exch}}$ for a normal and a cancer breast cell starting from the cell border to the border of the adjacent cell taking into account the typical size of the intercellular space for this tissue, namely about $0.2 - 0.3 \mu\text{m}$ for a normal cell and about $1.5 \mu\text{m}$ for a cancer cell⁵².

r_{eQ} was calculated according to equation (4) applied to glucose catabolism, while $r_{e\text{exch}}$ was calculated according to equation (5) applied to glucose catabolism (see Supplementary information, Section 3, equation (S32) and equation (S36), respectively). The parameters used in the numerical calculations are $k_B = 1.3805 \times 10^{-23} \text{ J/K}$, $N_{\text{mpr resp}} = 12$, the number of moles of the products of respiration, $N_{\text{mpr resp}} = 4$, the number of moles of the lactic acid fermentation reaction. In addition, like for the calculation of the rate of internal entropy density production we have taken $w_{\text{resp}} = 0.8$ ($w_{\text{ferm}} = 0.2$), the corresponding weights of the respiration (fermentation) processes for a normal cell and $w_{\text{resp}} = 0.1$ ($w_{\text{ferm}} = 0.9$) for a cancer cell³⁷⁻³⁹. The trend of r_{eQ} and $r_{e\text{exch}}$ for cancer cells is suitable to the observations^{29, 30, 32}.

As shown in Fig. 3a and b, r_{eQ} increases as a function of x for vanishing time and decreases with increasing time. $r_{e\text{exch}}$ displayed in Fig. 3c and d does not vary appreciably as a function of x and decreases with increasing time. The magnitude of r_{eQ} is much larger than the corresponding $r_{e\text{exch}}$ and this behaviour is enhanced in cancer cells where r_{eQ} is about one order of magnitude larger than in normal cells.

Discussion

According to the described model, we can draw important conclusions about the cell behaviour during glucose catabolism in terms of entropy production. While r_i is mainly due to matter exchanges, the greatest contribution to r_e comes from the heat irreversible release. Moreover, the amount of r_e is greater for a cancer cell and, due to the minor volume of a normal cell, r_i is on average greater for a normal cell. In contrast, r_e is greater in a cancer cell due to the larger contribution of r_{eQ} because of the prevalence of the dependence on the spatial coordinate with respect to that on the cell volume.

Note that we have applied the model to the particular case of cells belonging to breast tissue but it would be still valid if applied to different tissues characterized by other volume ratios between normal and cancer cells and easily extended to staminal cells that are of much smaller size.

As shown in Figs 2 and 3 for the epithelium breast normal and cancer cells, we have proved that $r(x, t) = r_i(x, t) + r_e(x, t)$ tends towards a minimum value with increasing time such that the cell reaches a state of global equilibrium in accordance with the minimum dissipation Prigogine's theorem. Moreover, looking especially at Fig. 2 displaying $r_i(x, t)$, the rate of entropy density production tends to its minimum value more slowly in a cancer cell with respect to a normal cell. This is a key point because it demonstrates that the tendency to stability or equivalently to global equilibrium is slower in a cancer cell. We can easily prove the fulfilment of the minimum dissipation Prigogine's theorem calculating $r(x, t)$ for the other irreversible reactions via equations (1-5). So far, there has been an application of this theorem to the uptake of the oxygen molecule in cells that is proportional to the released heat. However, albeit partially correct, this application does not take into account the

weight of glycolysis and of lactic acid fermentation or of other chemical reactions involving oxygen consumption. Instead, our model overcomes these limits encompassing quantitatively all those aspects and is not restricted to oxygen molecule consumption. We emphasize that the minimum dissipation of entropy is necessary to establish a condition compatible with the behaviour of Gibbs free energy in living systems because of the thermodynamic relation among free energy, enthalpy and entropy.

At the same time, we believe that the model, although giving general relations, represents a starting point and the results obtained are only an indication of what could occur in a specific calculation. Moreover, note that the calculated rates of entropy are not purely theoretical but strongly depend on consolidated experimental data like, for example, the frequency of occurrence of an irreversible process, the cellular volume and the average intercellular size. We wish that some experiments along this direction will be carried out to verify the importance of the calculations because we believe that measurements of the rate of entropy could bring new fundamental knowledge in the field shedding light on the important role played by metabolic, epigenetic and gene networks in living systems. For example, the number of moles of chemical species appearing in the main pathways like OXPHO and lactic acid fermentation can be carefully measured, e.g. *in vitro/in vivo* via imaging techniques by means of Nuclear Magnetic Resonance or Positive Emission Tomography (PET). This leads to a quantitative estimate of the rate of entropy due to mass transport opening the road for new measurements in cell biology. Note that the model can be applied to surfaces of internal parenchyma generalizing the rate of entropy relations found for a single cell to agglomerates of cells displayed with PET technique. On the other hand, measurements done by means of microcalorimetry technique may be employed to quantify the heat flow.

As the glucose catabolism is strongly correlated with the development of cancer and self-renewal processes, the described model, if validated by specific and real measures of glucose absorption^{29, 30} could introduce a new way to quantify the glucose catabolism in relation to the exchange of entropy occurring during this irreversible process.

Moreover, the interplay between the glucose uptake or production of lactate ion and the rate of entropy might be particularly important for clinical studies on cancer development and self-renewal process³⁸. It is also interesting to note that the developed formalism might be used also for electrophysiological processes with special regard to ionic fluxes. These processes have a crucial role in the development and progression of neoplastic processes and, in addition, the modulation of ionic currents might modulate the patterns of metabolic network^{42, 59}.

In summary, although the thermodynamics of irreversible processes introduced by De Donder and subsequently developed by Prigogine is, often, regarded as mainly theoretical and speculative, it could play a crucial role in describing a unified phenomenological paradigm of biological systems. More precisely, when modern biology faces the challenge of a systemic vision of life in terms of interactions among complex networks, the study of the rate of entropy represents a starting point able to reveal the phenomenological and unitary feature of life. Indeed, our results show that the study of the rate of entropy density production open new perspectives in modern biology giving a simple picture of irreversible processes in living systems.

Methods

Basic principles. Let us consider an open system (cell) that exchanges energy and matter with the environment. For a system in local equilibrium but not in global equilibrium, it is convenient to define an entropy density $s = S/V_{\text{cell}}$ with $s = s_i + s_e$ where s_i is the internal entropy density (subscript “i” indicates internal), s_e the external entropy density (subscript “e” indicates external) and V_{cell} the volume of the cell. The entropy density infinitesimal variation $ds = ds_i + ds_e$ includes the contribution ds_i related to internal irreversible processes and ds_e associated to the external exchanges of heat and matter with the intercellular environment. To fully describe the temporal evolution, it is useful to define the rate of entropy density production in a time interval dt in the form $r = ds_i/dt + ds_e/dt$. This quantity gives a direct measure of irreversible processes.

Rate of internal entropy density production. First, we express in a time interval dt the rate of internal entropy density production $r_i = \frac{ds_i}{dt}$ giving the amount of local increase of entropy inside a cell that can be regarded as a continuous system. In a compact form⁴³

$$r_i(\mathbf{x}, t) = \nabla \left(\frac{1}{T(\mathbf{x}, t)} \right) \cdot \mathbf{J}_u(\mathbf{x}, t) - \sum_{k=1}^N \nabla \left(\frac{\mu_k(\mathbf{x}, t)}{T(\mathbf{x}, t)} \right) \cdot \mathbf{J}_{Dk}(\mathbf{x}, t) + \frac{1}{T(\mathbf{x}, t)} \sum_{j=1}^M A_j(\mathbf{x}, t) v_j \quad (6)$$

Here, the first term on the second member is associated with the internal flow $\mathbf{J}_u = \mathbf{J}_Q + \sum_{k=1}^N \mu_k \mathbf{J}_{Dk}$, with N the number of chemical species, getting contributions from irreversible heat flow \mathbf{J}_Q and diffusion flow \mathbf{J}_{Dk} and driven by the heat thermodynamic force $\mathbf{F}_u(\mathbf{x}, t) = \nabla(T(\mathbf{x}, t))^{-1}$. The second term is related to the diffusion flow \mathbf{J}_{Dk} and is driven by the matter thermodynamic force $\mathbf{F}_k(\mathbf{x}, t) = \nabla \left(\frac{\mu_k(\mathbf{x}, t)}{T(\mathbf{x}, t)} \right)$ with μ_k the chemical potential of the k th chemical species.

Finally, the last term is associated with irreversible reactions being M the number of chemical reactions with the thermodynamic force represented by the affinity $A_j(\mathbf{x}, t) = - \sum_{k=1}^N \nu_{jk} \mu_k(\mathbf{x}, t)$ with ν_{jk} the stoichiometric coefficients, and the corresponding flow by the velocity of the j th reaction $v_j = \frac{1}{V_{\text{cell}}} \frac{d\xi_j}{dt}$ with $d\xi_j$ the variation of the j th degree of advancement.

Rate of external entropy density production. We express, in the same time interval dt the rate of external entropy density production $r_e = \frac{ds_e}{dt}$ giving the amount of local increase of entropy outside the cell corresponding to the intercellular environment. In its general form

$$r_e(\mathbf{x}, t) = \frac{1}{T_{ic}(\mathbf{x}, t)} \frac{1}{V_{cell}} \frac{dQ}{dt} - \frac{1}{T_{ic}(\mathbf{x}, t)} \sum_{k=1}^{N_{pr}} \mu_k(\mathbf{x}, t) \frac{d_e N_{mk}}{dt} \quad (7)$$

here, $\frac{1}{V_{cell}} \frac{dQ}{dt} = \frac{du}{dt} + \frac{1}{V_{cell}} p \frac{dV}{dt}$ according to the first principle of thermodynamics. $dQ = dU + pdV$ with dQ the infinitesimal heat transfer, $du = \frac{1}{V} dU$ the infinitesimal variation of the internal energy density u (dU is the infinitesimal variation of the internal energy U), p the pressure and dV the infinitesimal variation of the volume V . In addition, $T_{ic}(\mathbf{x}, t)$ is the intercellular temperature distribution and $d_e N_{mk}$ the variation of the number of moles of the k th chemical species with N_{pr} the number of products of the irreversible reaction (“pr” indicates products) due to exchange of matter with the intercellular environment.

The first term on the second member expresses the heat flow outside the cell, while the second one results from the exchange of matter with the intercellular environment.

Diffusion equations. In order to find the heat and mass flow appearing in the expression of the RIEDP given in equations (1) and (2), we employ the well-known heat and mass transport equations. We consider a rectangular frame xyz with the origin in the center of the cell and we suppose that the flow direction is along x (see Fig. 1).

Concerning the heat diffusion, it is mainly due to a conduction transport neglecting the convection transport present to a much lesser extent inside a typical cell and the term of heat source. Hence, it is

$$\frac{\partial T(\mathbf{x}, t)}{\partial t} = \kappa \nabla^2 T(\mathbf{x}, t) \quad (8)$$

where the solution $T(\mathbf{x}, t)$ is the temperature distribution function depending on both spatial and time variable, $\kappa = \frac{K}{c_s \rho}$ is the thermal diffusivity ($\text{m}^2 \text{s}^{-1}$) with K the thermal conductivity expressed in $\text{J m}^{-1} \text{s}^{-1} \text{K}^{-1}$ and supposed uniform, c_s the specific heat expressed in $\text{J Kg}^{-1} \text{K}^{-1}$ and ρ the density expressed in Kg m^{-3} . The flow $J_Q(\mathbf{x}, t)$ is proportional to the spatial derivative of $T(\mathbf{x}, t)$.

Analogously, the mass transport equation or Fick’s second diffusion law reads

$$\frac{\partial n(\mathbf{x}, t)}{\partial t} = D \nabla^2 n(\mathbf{x}, t) \quad (9)$$

where, the solution $n(\mathbf{x}, t)$ is the concentration of molecules, a distribution function depending both on spatial and time variables and D is the diffusion coefficient ($\text{m}^2 \text{s}^{-1}$) supposed uniform. The flow $J_D(\mathbf{x}, t)$ is proportional to the spatial derivative of $n(\mathbf{x}, t)$.

References

- Prigogine, I., Mayné, F., George, C. & De Haan, M. Microscopic theory of irreversible processes. *Proc. Natl. Acad. Sci.* **74**, 4152–456 (1977).
- Lucia, U. The Gouy-Stodola Theorem in Bioenergetic Analysis of Living Systems (Irreversibility in Bioenergetics of Living Systems). *Energies* **7**, 5717 (2014).
- Zotin, A. A. & Zotin, A. I. Phenomenological theory of ontogenesis. *Int. J. Dev. Biol.* **41**, 917–921 (1997).
- Luisi, P. L. The minimal autopoietic unit. *Orig. Life Evol. Biosph.* **44**, 335–338 (2014).
- Keller, M. A., Turchyn, A. V. & Ralsler, M. Non-enzymatic glycolysis and pentose phosphate pathway-like reactions in a plausible Archean ocean. *Mol. Syst. Biol.* **10**, 725 (2014).
- Nicolis, G. & Prigogine, I. *Self-organization in non-equilibrium systems* (Wiley, 1977).
- Clausius, R. *The Mechanical Theory of Heat*. London (Taylor and Francis, 1867).
- Huang, K. *Statistical mechanics* (Wiley, 1987).
- Wong, C. C., Qian, Y. & Yu, J. Interplay between epigenetics and metabolism in oncogenesis: mechanisms and therapeutic approaches. *Oncogene* **36**, 1–16 (2017).
- Peng, M. *et al.* Aerobic glycolysis promotes T helper 1 cell differentiation through an epigenetic mechanism. *Science* **354**, 481–484 (2016).
- Moussaieff, A. *et al.* Glycolysis-mediated changes in acetyl-CoA and histone acetylation control the early differentiation of embryonic stem cells. *Cell Metab.* **21**, 392–402 (2015).
- Gut, P. & Verdin, E. The nexus of chromatin regulation and intermediary metabolism. *Nature* **502**, 489–498 (2013).
- Hino, S., Nagaoka, K. & Nakao, M. Metabolism-epigenome crosstalk in physiology and diseases. *J. Hum. Genet.* **58**, 410–415 (2013).
- Banerji, C. R. *et al.* Cellular network entropy as the energy potential in Waddington’s differentiation landscape. *Sci. Rep.* **3**, 3039 (2013).
- Himeoka, Y. & Kaneko, K. Entropy production of a steady-growth cell with catalytic reactions. *Phys. Rev. E* **90**, 042714 (2014).
- Vilar, J. M. G. Entropy of Leukemia on Multidimensional Morphological and Molecular Landscapes. *Phys. Rev. X* **4**, 021038 (2014).
- Ridden, S. J., Chang, H. H., Zygalakis, K. C. & MacArthur, B. D. Entropy, Ergodicity, and Stem Cell Multipotency. *Phys. Rev. Lett.* **115**, 208103 (2015).
- Banerji, C. R., Severini, S. & Teschendorff, A. E. Network transfer entropy and metric space for causality inference. *Phys. Rev. E* **87**, 052814 (2013).
- Funo, K., Shitara, T. & Ueda, M. Work fluctuation and total entropy production in nonequilibrium processes. *Phys. Rev. E* **94**, 062112 (2016).
- Warburg, O. On respiratory impairment in cancer cells. *Science* **124**, 269–270 (1956).
- Pacini, N. & Borziani, F. Cancer stem cell theory and the warburg effect, two sides of the same coin? *Int. J. Mol. Sci.* **15**, 8893–8930 (2014).
- Pacini, N. & Borziani, F. Oncostatic-Cytoprotective Effect of Melatonin and Other Bioactive Molecules: A Common Target in Mitochondrial Respiration. *Int. J. Mol. Sci.* **17**, 344 (2016).
- Wang, P., Wan, W., Xiong, S. L., Feng, H. & Wu, N. Cancer stem-like cells can be induced through dedifferentiation under hypoxic conditions in glioma, hepatoma and lung cancer. *Cell Death Dis.* **3**, 16105 (2017).
- Qian, X., Hu, J., Zhao, J. & Chen, H. ATP citrate lyase expression is associated with advanced stage and prognosis in gastric adenocarcinoma. *Int. J. Clin. Exp. Med.* **8**, 7855–7860 (2015).
- Li, X. *et al.* Metabolic reprogramming is associated with flavopiridol resistance in prostate cancer DU145 cells. *Sci. Rep.* **7**, 5081 (2017).
- Lévy, P. & Bartosch, B. Metabolic reprogramming: a hallmark of viral oncogenesis. *Oncogene* **35**, 4155–4164 (2016).

27. Baumann, K. Stem cells: A metabolic switch. *Nat. Rev. Mol. Cell Biol.* **2**, 64–65 (2013).
28. Ito, K. & Suda, T. Metabolic requirements for the maintenance of self-renewing stem cells. *Nat. Rev. Mol. Cell Biol.* **4**, 243–256 (2014).
29. Marinelli, B. *et al.* Prognostic value of FDG PET/CT-based metabolic tumor volumes in metastatic triple negative breast cancer patients. *Am. J. Nucl. Med. Mol. Imaging* **6**, 120–127 (2016).
30. Grootjans, W. *et al.* PET in the management of locally advanced and metastatic NSCLC. *Nat. Rev. Clin. Oncol.* **12**, 395–407 (2015).
31. Wulaningsih, W. *et al.* Serum lactate dehydrogenase and survival following cancer diagnosis. *Br. J. Cancer* **113**, 1389–1396 (2015).
32. Lucia, U. & Grisolia, G. Second law efficiency for living cells. *Front. Biosci.* **9**, 270–275 (2017).
33. Ozernyuk, N. D., Zotin, A. I. & Yurowitzky, Y. G. Deviation of the living system from the stationary state during oogenesis. *Wilhelm Roux Archiv.* **172**, 66–74 (1973).
34. Lucia, U. Bioengineering Thermodynamics: An Engineering Science for Thermodynamics of Biosystems. *IJoT* **18**, 254–265 (2015).
35. Lucia, U. Carnot efficiency: Why? *Physica A* **392**, 3513–3517 (2013).
36. Lucia, U. Electromagnetic waves and living cells: A kinetic thermodynamic approach. *Physica A* **461**, 577–585 (2013).
37. Daniele, S. *et al.* Lactate dehydrogenase-A inhibition induces human glioblastoma multiforme stem cell differentiation and death. *Sci. Rep.* **5**, 15556 (2015).
38. Son, M. J. *et al.* Upregulation of mitochondrial NAD⁺ levels impairs the clonogenicity of SSEA1⁺ glioblastoma tumor-initiating cells. *Exp. Mol. Med.* **49**, e344 (2017).
39. Sancho, P., Barneda, D. & Heeschen, C. Hallmarks of cancer stem cell metabolism. *Br. J. Cancer* **114**, 1305–1312 (2016).
40. Scott, C. B. A Primer for the Exercise and Nutrition Sciences (Humana Press, 2008).
41. Lucia, U. *et al.* Constructal thermodynamics combined with infrared experiments to evaluate temperature differences in cells. *Sci. Rep.* **5**, 11587 (2015).
42. Lucia, U., Ponzetto, A. & Deisbock, S. T. Constructal approach to cell membranes transport: Amending the ‘Norton-Simon’ hypothesis for cancer treatment. *Sci. Rep.* **6**, 19451 (2016).
43. Okabe, C. *et al.* Intracellular temperature mapping with a fluorescent polymeric thermometer and fluorescence lifetime imaging microscopy. *Nat. Comm.* **3**, 1714 (2012).
44. Kase, K. & Hahn, G. M. Differential heat response of normal and transformed human cells in tissue culture. *Nature* **255**, 228–230 (1975).
45. Ohtake, M. Hyperthermia and chemotherapy using Fe (Salen) nanoparticles might impact glioblastoma treatment. *Sci. Rep.* **7**, 42783 (2017).
46. Kondepudi, D. & Prigogine, I. Modern thermodynamics: From heat engines to dissipative structures (Wiley, 2015).
47. Dabbs, D. J. *et al.* Molecular alterations in columnar cell lesions of the breast. *Mod. Pathol.* **19**, 344–349 (2006).
48. Iden, S. & Collard, J. G. Crosstalk between small GTPases and polarity proteins in cell polarization. *Nat. Rev. Mol. Cell Biol.* **9**, 846–859 (2008).
49. Lim, C. S. *et al.* Measurement of the nucleus area and nucleus/cytoplasm and mitochondria/nucleus ratios in human colon tissues by dual-colour two-photon microscopy imaging. *Sci. Rep.* **5**, 18521 (2015).
50. Deng, D. *et al.* Molecular basis of ligand recognition and transport by glucose transporters. *Nature* **526**, 391–396 (2015).
51. Geltmeier, A. *et al.* Characterization of dynamic behaviour of MCF7 and MCF10A cells in ultrasonic field using modal and harmonic analyses. *PLoS One* **10**, e0134999 (2015).
52. Ozzello, L. Ultrastructure of human mammary carcinoma cells *in vivo* and *in vitro*. *J. Natl. Cancer Inst.* **48**, 1043–1050 (1972).
53. De la Fuente, I. M. *et al.* On the dynamics of the adenylate energy system: homeorhesis vs homeostasis. *PLoS One* **9**, e108676 (2014).
54. Apps, D. K. & Nairn, A. C. The equilibrium constant and the reversibility of the reaction catalysed by nicotinamide-adenine dinucleotide kinase from pigeon liver. *Biochem. J.* **167**, 87–93 (1977).
55. Mitchell, P. Aspects of the chemiosmotic hypothesis. *Biochem. J.* **116**, 5P–6P (1970).
56. Chiang, E. Y. *et al.* Potassium channels Kv1.3 and KCa3.1 cooperatively and compensatorily regulate antigen-specific memory T cell functions. *Nat. Comm.* **8**, 14644 (2017).
57. Beck, W. S. A kinetic analysis of the glycolytic rate and certain glycolytic enzymes in normal and leukemic leucocytes. *J. Biol. Chem.* **216**, 333–350 (1955).
58. Sánchez-Danés, A. *et al.* Defining the clonal dynamics leading to mouse skin tumour initiation. *Nature* **536**, 298–303 (2016).
59. Lucia, U. Bioengineering thermodynamics of biological cells. *Theor. Biol. Med. Model.* **12**, 29 (2015).

Acknowledgements

This work was partially supported by National Group of Mathematical Physics (GNFM-INdAM). We are grateful to S. Gangi, A. Strazzanti and F. Borziani for helpful discussion and kind support in this research activity. We thank Domenico Romolo for his graphical support in making Fig. 1a. This work is dedicated to the memory of Ilya Prigogine in occasion of his 100th birth anniversary.

Author Contributions

R.Z. developed the theoretical model and performed numerical calculations. N.P. conceived the problem. R.Z., N.P. and M.C. wrote the paper with inputs from G.F. All authors contributed to the analysis of the results.

Additional Information

Supplementary information accompanies this paper at doi:10.1038/s41598-017-09530-5

Competing Interests: The authors declare that they have no competing interests.

Publisher's note: Springer Nature remains neutral with regard to jurisdictional claims in published maps and institutional affiliations.



Open Access This article is licensed under a Creative Commons Attribution 4.0 International License, which permits use, sharing, adaptation, distribution and reproduction in any medium or format, as long as you give appropriate credit to the original author(s) and the source, provide a link to the Creative Commons license, and indicate if changes were made. The images or other third party material in this article are included in the article's Creative Commons license, unless indicated otherwise in a credit line to the material. If material is not included in the article's Creative Commons license and your intended use is not permitted by statutory regulation or exceeds the permitted use, you will need to obtain permission directly from the copyright holder. To view a copy of this license, visit <http://creativecommons.org/licenses/by/4.0/>.

© The Author(s) 2017

SUPPLEMENTARY INFORMATION

Rate of entropy model for irreversible processes in living systems

R. Zivieri^{1,2}, N. Pacini³, G. Finocchio², M. Carpentieri⁴

¹Department of Physics and Earth Sciences and Consorzio Nazionale Interuniversitario per le Scienze Fisiche della Materia, Unit of Ferrara, University of Ferrara, via G. Saragat 1, Ferrara I-44122, Italy

²Department of Mathematical and Computer Sciences, Physical Sciences and Earth Sciences, University of Messina, V.le F. D'Alcontres, 31, 98166, Messina, Italy

³Department of General Surgery, Section of Senology, University Hospital Company, Policlinico Vittorio Emanuele, via S. Citelli 6, 95124, Catania, Italy

⁴Department of Electrical and Information Engineering, Politecnico di Bari, via E. Orabona 4, Bari I-70125, Italy

1. OVERVIEW

We restrict ourselves to the study of the thermodynamics in the single cell representing an open thermodynamic system. Since we are dealing with phenomena taking place locally and under conditions of local equilibrium inside and outside a typical cell, all intensive and extensive thermodynamic variables have a space and time dependence [S1]. On this basis, it is useful to define the rate of entropy density production, $r = r_i + r_e$, where r_i is the rate of internal entropy density production (RIEDP) and r_e the rate of external entropy density production (REEDP). Starting from the definition of the entropy density $s = \frac{S}{V_{\text{cell}}}$ with $s = s_i + s_e$ where s_i is the internal entropy density, s_e the external entropy density and V_{cell} the volume of the cell it is possible to compute r .

In the next two sections, we give the details about the calculation of r_i and r_e , respectively valid for any irreversible processes occurring in a cell, either normal or cancer. The calculation lies on thermodynamic arguments combined with heat and mass transport equations. The expressions are general and valid for any irreversible chemical process and we then apply them to glucose catabolism.

To calculate the rate of entropy density production, for the sake of convenience and without loss of generality, we represent the cell (either normal or cancer) as a cube of volume $V_{\text{cell}} = L^3$ taking as reference the breast epithelium tissue. Here, L is the average size with $L = 10 \mu\text{m}$ for a typical normal cell and $L = 20 \mu\text{m}$ for a cancer cell [S2] and we assume that the flows occur mainly along the x direction within a 1D model (see Fig. 1 in the main text). In the numerical calculations shown in the following we assume that all irreversible processes take place at $x = L/2$ and for values of y and z corresponding to the region of the cytoplasm where glucose catabolism occurs (see the main text for more details).

To describe the glucose catabolism we recall the two reactions described in detail in the main text, namely the respiration process and the lactic acid fermentation process involving glucose ($\text{C}_6\text{H}_{12}\text{O}_6$) catabolism. The respiration process is summarized as $\text{C}_6\text{H}_{12}\text{O}_6 + 6\text{O}_2 \rightarrow 6\text{CO}_2 + 6\text{H}_2\text{O}$ leading to the formation of carbon dioxide (CO_2) and water (H_2O). The lactic acid fermentation process leads to the formation of two lactic acid ions ($\text{C}_3\text{H}_5\text{O}_3^-$) and two protons (H^+) and is summarized in the

simple form $C_6H_{12}O_6 \rightarrow 2 C_3H_5 O_3^- + 2 H^+$ [S3, S4] (for a more detailed discussion on this point see the main text).

2. RATE OF INTERNAL ENTROPY DENSITY PRODUCTION

We define the space and time dependent RIEDP $r_i(\mathbf{x}, t) = \frac{ds_i(\mathbf{x}, t)}{dt}$ (with $\mathbf{x} = (x, y, z)$ and t the time) giving the amount of local increase of entropy in continuous thermodynamic systems. In our special case, we consider a cell (either normal or cancer) and the RIEDP associated to irreversible processes occurring inside it.

In order to do that, we recall its general expression in terms of heat flow and mass flow (see Methods):

$$r_i(\mathbf{x}, t) = \nabla \left(\frac{1}{T(\mathbf{x}, t)} \right) \cdot \mathbf{J}_u(\mathbf{x}, t) - \sum_{k=1}^N \nabla \left(\frac{\mu_k(\mathbf{x}, t)}{T(\mathbf{x}, t)} \right) \cdot \mathbf{J}_{Dk}(\mathbf{x}, t) + \frac{1}{T(\mathbf{x}, t)} \sum_{j=1}^M A_j(\mathbf{x}, t) v_j \quad (S1)$$

Here, $\nabla \left(\frac{1}{T(\mathbf{x}, t)} \right)$ is the thermodynamic force leading to the internal energy flow $\mathbf{J}_u = \mathbf{J}_Q + \sum_{k=1}^N u_k \mathbf{J}_{Dk}$ with \mathbf{J}_Q the heat flow, u_k the partial molar energy and \mathbf{J}_{Dk} the diffusion flow of the k th chemical species with N the number of chemical species. In particular, $u_k = \left(\frac{\partial u}{\partial n_{mk}} \right)_T$ is expressed in J/mole with u the energy density expressed in J/m³, $n_{mk} = \frac{N_{mk}}{V}$ the number of moles per unit volume of the k th species with N_{mk} the number of moles. Instead, $\nabla \left(\frac{\mu_k(\mathbf{x}, t)}{T(\mathbf{x}, t)} \right)$ is the k th thermodynamic force giving rise to the diffusion flow $\mathbf{J}_{Dk}(\mathbf{x}, t)$. Finally, $A_j(\mathbf{x}, t)$ is the affinity of the j th chemical reaction and v_j is the velocity of reaction with M the number of chemical reactions.

It is possible to identify three different contributions to the RIEDP: 1) the one associated to heat transport; 2) the one related to molecules diffusion and 3) the one due to irreversible chemical reactions. The second and third contributions are those due to mass transport. The heat transport is

caused by the temperature gradient inside the human cell. Within this model, we do not include the term $\nabla\left(\frac{1}{T(\mathbf{x},t)}\right)\cdot\sum_{k=1}^N u_k \mathbf{J}_{Dk}(\mathbf{x},t)$ that expresses the thermodynamic force due to temperature distribution gradient inside the cell and the corresponding mass flow. In this way, we do not take into account the contribution to the rate of internal entropy density caused by diffusion of chemical species whose flow results from the temperature distribution gradient.

A. RATE OF INTERNAL ENTROPY PRODUCTION ASSOCIATED TO HEAT TRANSPORT

First, we derive the RIEDP associated to heat transport related to the flow $\mathbf{J}_Q(\mathbf{x},t)$ within our model. In its general form:

$$r_{iQ}(\mathbf{x},t) = \mathbf{F}_Q(\mathbf{x},t) \cdot \mathbf{J}_Q(\mathbf{x},t) \quad (\text{S2})$$

Here, $\mathbf{F}_Q(\mathbf{x},t) = \nabla\left(\frac{1}{T(\mathbf{x},t)}\right)$ is the thermodynamic force. In our 1D model, without loss of generality, flows are assumed along x ; hence, $\mathbf{x} = (x, 0, 0)$, $\nabla \rightarrow \frac{\partial}{\partial x} \hat{i}$, $T(\mathbf{x},t) \rightarrow T(x,t)$ and $\mathbf{J}_Q = (J_Q, 0, 0)$. Heat flow occurs symmetrically with respect to $x = L/2$ along the two directions (x and $-x$).

To calculate the heat flow, we make the assumption that heat diffusion is mainly due to a conduction transport neglecting, in a first approximation, the convection transport present to a much lesser extent inside a typical cell. The heat transport equation in the 1D case, neglecting the term of heat source, takes the well-known form:

$$\frac{\partial T(x,t)}{\partial t} = \kappa \frac{\partial^2 T(x,t)}{\partial x^2} \quad (\text{S3})$$

Here, the solution to Equation (S3) $T(x,t)$ is the temperature distribution function depending both on spatial and time variable, and, for a given material, $\kappa = K/(c_s \rho)$ is the thermal diffusivity in m^2/s with K the thermal conductivity in $\text{J}/(\text{m s K})$, c_s the specific heat in $\text{J}/(\text{Kg K})$ and ρ the density in $\text{Kg}/$

m^3 . Both K and κ are assumed uniform throughout the cell. We impose the following initial and boundary conditions on the temperature distribution:

$$\begin{cases} T(x,0) = T_0 & \text{for } 0 \leq x \leq L & \text{initial condition} \\ T(0,t) = T(L,t) = 0 & \text{for } t > 0 & \text{boundary conditions} \end{cases} \quad (\text{S4})$$

This choice is not restrictive because the temperature vanishes only exactly at the cell border due to the boundary conditions corresponding to the cell membrane and has a weak dependence on x inside the cell. However, note that the temperature on the cell membrane is not zero as inferred from the expression of the temperature distribution in the intercellular environment (see paragraph B for details) obtained in the absence of boundary conditions. The solution to equation (S3) taking into account the initial and boundary conditions expressed by equation (S4) reads

$$T(x,t) = \frac{4T_0}{\pi} \sum_{n=1}^{\infty} \left(\frac{\sin \left[(2n-1) \frac{\pi}{L} x \right]}{2n-1} e^{-\kappa(2n-1)^2 \frac{\pi^2}{L^2} t} \right) \quad (\text{S5})$$

A graphical solution to equations (S4) and (S5) of the temperature distribution (in Kelvin, K) inside the cell is shown in Fig. S1a and Fig.S1b as a function of x and of t with t ranging from 0 to 1000 μs , a typical cell time interval. In the numerical calculations, we have taken the initial temperature $T_0 = 310$ K and, taking into account that the cytoplasm is mainly composed by water, we have used the thermal diffusivity of water, viz. $\kappa_{\text{H}_2\text{O}} = 0.143 \times 10^{-6} \text{ m}^2/\text{s}$. The temperature is almost uniform and, on average, about T_0 especially for the initial instant of times (see Fig.S1c and Fig.S1d). The temperature vanishes only at the border corresponding to the cellular membrane for $t > 0$ because of the boundary condition of equation (S4).

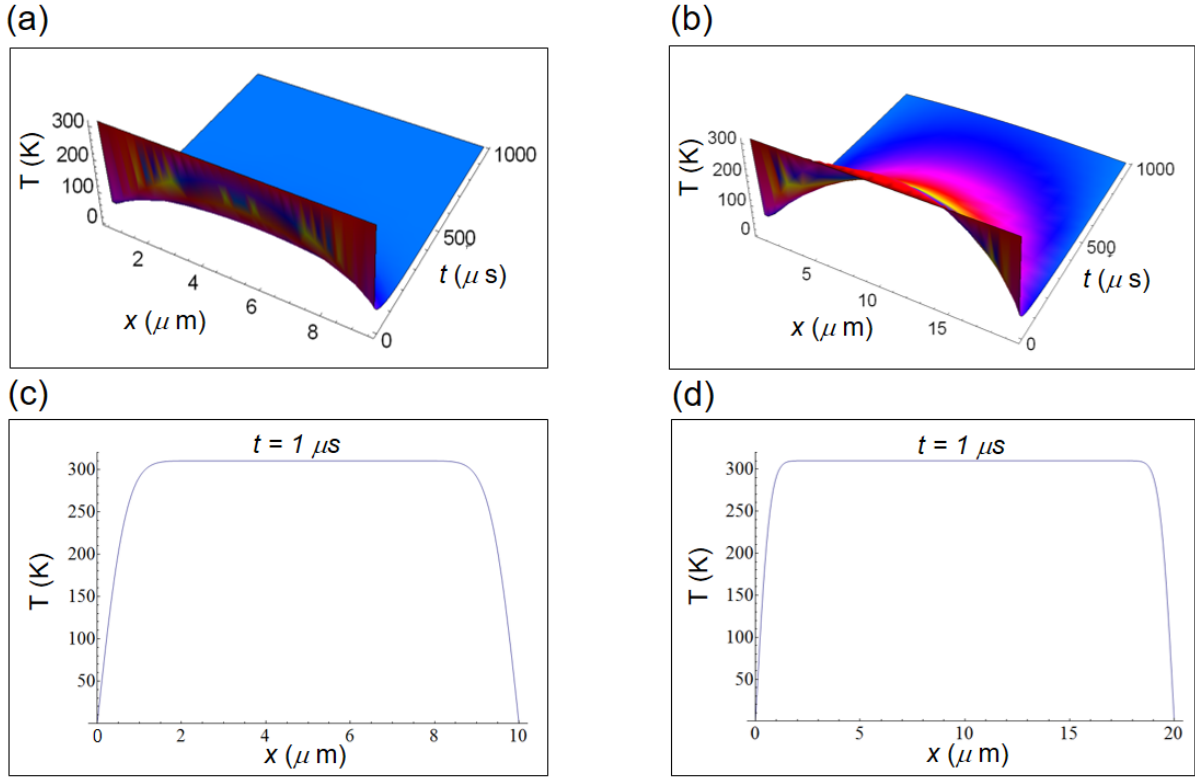


Figure S1. Temperature distribution inside a human cell according to equations (S4) and (S5). (a) Temperature distribution inside a normal cell as a function of the spatial coordinate and time. (b) Temperature distribution inside a cancer cell as a function of the spatial coordinate and time. (c) Temperature as a function of the spatial coordinate in a normal cell. (d) Temperature as a function of the spatial coordinate in a cancer cell.

For the 1D case $\mathbf{F}_Q = (F_Q, 0, 0)$ with $\mathbf{F}_Q(x, t) = \frac{\partial}{\partial x} \left[(T(x, t))^{-1} \right] e^{-\frac{t}{\tau}} \hat{i}$ expressed in $1/(\text{m K})$ where an exponential time decay depending on a typical decay time τ has been included to describe the time evolution of the force. Hence, by inserting the solution to heat equation given in equation (S5), we get

$$\mathbf{F}_Q(x, t) = -\frac{\pi^2}{4} \frac{1}{T_0} \frac{1}{L} \frac{\sum_{n=1}^{\infty} \left(\cos \left[(2n-1) \frac{\pi}{L} x \right] e^{-\kappa(2n-1)^2 \frac{\pi^2}{L^2} t} \right) e^{-\frac{t}{\tau}}}{\left(\sum_{n=1}^{\infty} \frac{1}{2n-1} \left(\sin \left[(2n-1) \frac{\pi}{L} x \right] e^{-\kappa(2n-1)^2 \frac{\pi^2}{L^2} t} \right) \right)^2} \hat{i} \quad (\text{S6})$$

Fig. S2 displays the force expressed in equation (S6) for a normal and a cancer cell with $\tau = 10^{-4}$ s a typical cell decay time. In the interval $0 \leq x \leq L/2$ we have taken the modulus of \mathbf{F}_Q to have the force positive in the whole interval. The force becomes greater passing from the center to the border and reduces its magnitude with increasing time. This force is only due to the internal temperature distribution and it is the same for all chemical species.

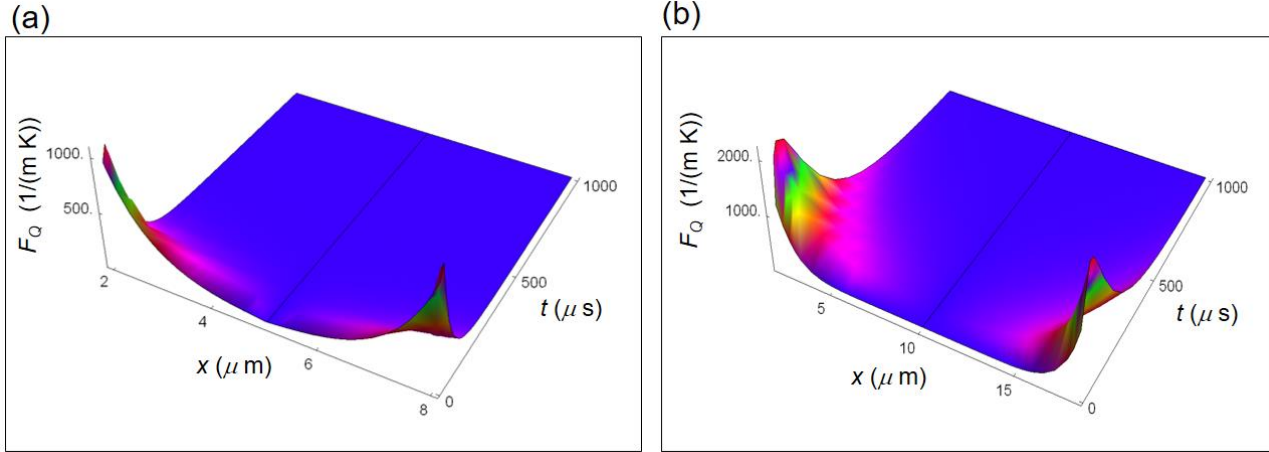


Figure S2. Force associated to internal heat flow calculated by means of equation (S6) as a function of the spatial coordinate and of time. (a) Force inside a normal cell. (b) Force inside a cancer cell.

Within the 1D model, the heat flow per unit time and area expressed in $\text{J}/(\text{m}^2 \text{s})$ is $\mathbf{J}_Q = (J_Q, 0, 0)$ with $J_Q = \frac{1}{A} \frac{dX_Q}{dt}$, dX_Q the heat flow and A is the cell area. According to Fourier law, the heat flow per unit time and per unit area along x is $J_Q(x, t) = -K \frac{\partial T(x, t)}{\partial x}$. The minus sign on the second member only indicates that heat flows from the region at higher temperature corresponding to the cell centre to the region at lower temperature close to the cell membrane, namely in the direction along which the temperature decreases (in this case it is symmetrical along $+x$ and $-x$). Explicitly

$$\mathbf{J}_Q(x, t) = -4 p K T_0 \frac{1}{L} \sum_{n=1}^{\infty} \left[\cos \left[(2n-1) \frac{\pi}{L} x \right] e^{-\kappa(2n-1)^2 \frac{\pi^2}{L^2} t} \right] \hat{i} \quad (\text{S7})$$

Here, p denotes the frequency of occurrence of the irreversible reaction. In Fig. S3, we display the bidirectional heat flow per unit time and area given in equation (S7) for both the normal and the cancer cell referred to glucose catabolism. For $0 \leq x \leq L/2$ we have plotted the modulus of the heat flow to have J_Q positive in the whole interval. In the numerical calculations we have taken $K = 0.600$

$J/(\text{m s K})$ and, for the case of glucose catabolism, $p = 0.90$ for cancer cells and $p = 0.85$ for normal cells [S5] (see the main text for more details). The trend of J_Q is symmetric with respect to the centre for the two types of cells, is less sharp for a cancer cell especially for t ranging between 0 and $100 \mu\text{s}$ and tends to zero with increasing time.

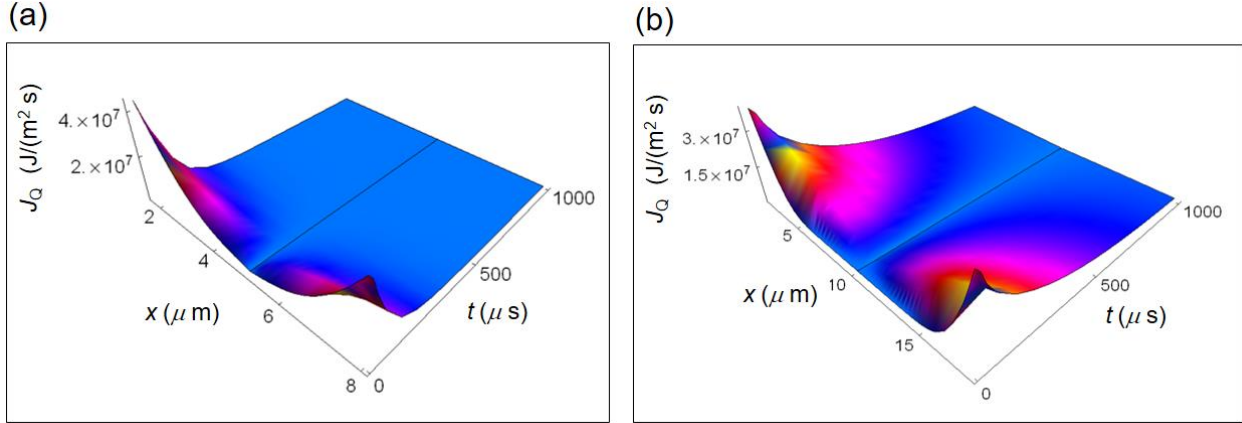


Figure S3. Internal heat flow per unit time and area calculated according to equation (S7) plotted as a function of the spatial coordinate and of time. (a) Heat flow inside a normal cell. (b) Heat flow inside a cancer cell.

The RIEDP due to the heat flow and expressed in $J/(\text{m}^3 \text{K s})$, via equation (S6) and equation (S7), is

$$r_{iQ}(x,t) = p K \frac{\pi^2}{L^2} \frac{\left[\sum_{n=1}^{\infty} \left(\cos \left[(2n-1) \frac{\pi}{L} x \right] e^{-\kappa(2n-1)^2 \frac{\pi^2}{L^2} t} \right) \right]^2}{\left[\sum_{n=1}^{\infty} \left(\frac{1}{2n-1} \sin \left[(2n-1) \frac{\pi}{L} x \right] e^{-\kappa(2n-1)^2 \frac{\pi^2}{L^2} t} \right) \right]^2} e^{-\frac{t}{\tau}} \quad (\text{S8})$$

From equation (S8), it turns out that $r_{iQ}(x,t) \geq 0$. Equation (S8) is equation (1) of the main text.

Note that both the numerator and the denominator can be written in terms of the product of two identical series, namely

$$\left[\sum_{n=1}^{\infty} \left(\cos \left[(2n-1) \frac{\pi}{L} x \right] e^{-\kappa(2n-1)^2 \frac{\pi^2}{L^2} t} \right) \right]^2 = \sum_{n=1}^{\infty} \left(\cos \left[(2n-1) \frac{\pi}{L} x \right] e^{-\kappa(2n-1)^2 \frac{\pi^2}{L^2} t} \right) \times \sum_{n=1}^{\infty} \left(\cos \left[(2n-1) \frac{\pi}{L} x \right] e^{-\kappa(2n-1)^2 \frac{\pi^2}{L^2} t} \right)$$

$$\left[\sum_{n=1}^{\infty} \left(\frac{1}{2n-1} \sin \left[(2n-1) \frac{\pi}{L} x \right] e^{-\kappa(2n-1)^2 \frac{\pi^2}{L^2} t} \right) \right]^2 = \sum_{n=1}^{\infty} \left(\frac{1}{2n-1} \sin \left[(2n-1) \frac{\pi}{L} x \right] e^{-\kappa(2n-1)^2 \frac{\pi^2}{L^2} t} \right) \times \sum_{n=1}^{\infty} \left(\frac{1}{2n-1} \sin \left[(2n-1) \frac{\pi}{L} x \right] e^{-\kappa(2n-1)^2 \frac{\pi^2}{L^2} t} \right) \quad (\text{S9})$$

B. RATE OF INTERNAL ENTROPY DENSITY PRODUCTION DUE TO DIFFUSION PROCESS

From equation (S1), we express the contribution to RIEDP related to diffusion process via the term

$$r_{iD}(\mathbf{x}, t) = - \sum_{k=1}^N \mathbf{F}_k^{(2)}(\mathbf{x}, t) \cdot \mathbf{J}_{Dk}(\mathbf{x}, t) \quad (\text{S10})$$

The thermodynamic force that gives rise to matter (chemical species) flow is

$$\mathbf{F}_k^{(2)}(\mathbf{x}, t) = \nabla \left(\frac{\mu_k(\mathbf{x}, t)}{T(\mathbf{x}, t)} \right). \quad \mathbf{F}_k^{(2)}(\mathbf{x}, t) \text{ is a new force depending on the chemical species } k \text{ that}$$

determines diffusion flow and is expressed in J/(mole m K). Within this description in terms of

densities, in chemical reactions $u_k = \left(\frac{\partial u}{\partial n_{mk}} \right)_T$ is the partial molar energy of the k th chemical species

expressed in J/mole with u the energy density expressed in J/m³, $n_{mk} = N_{mk}/V$ the number of moles per unit volume of the k th species with N_{mk} the number of moles. Instead, the chemical potential of

the k th chemical species is determined as $\mu_k(\mathbf{x}, t) = \left(\frac{\partial g(\mathbf{x}, t)}{\partial n_{mk}} \right)_{T,P}$ where $g = G/V$ is the Gibbs free

energy density at constant pressure and G is the Gibbs free energy. According to its general definition given above, the chemical potential depends on the temperature and on the pressure.

$$\text{For the 1D case, } \mathbf{F}_k^{(2)} = (F_k^{(2)}, 0, 0) \text{ with } F_k^{(2)} = \frac{\partial}{\partial x} \left(\frac{\mu_k(x, t)}{T(x, t)} \right) \hat{i}. \text{ Here, } \mu_k(x, t) = u_k e^{-(|x-L/2|/L + t/\tau)}$$

is the time and space dependent chemical potential of the k th chemical species with τ a typical cell decay time; u_k is the chemical potential calculated at $x = L/2$, where it is assumed that the glucose catabolism takes place, that is equal to the partial molar energy. According to this form, the chemical

potential decreases passing from the center to the border of the cell and decreases with increasing time. For every irreversible reaction and for every chemical species $\mathbf{F}_k^{(2)}(x, t)$ is

$$\mathbf{F}_k^{(2)}(x, t) = -\frac{\pi^2}{4} \frac{1}{T_0} \frac{1}{L} \times \left(\frac{u_k e^{-(|x-L/2|/L+t/\tau)} \left(\pm \frac{1}{\pi} \sum_{n=1}^{\infty} \left(\frac{1}{2n-1} \sin \left[(2n-1) \frac{\pi}{L} x \right] e^{-\kappa(2n-1)^2 \frac{\pi^2}{L^2} t} \right) + \sum_{n=1}^{\infty} \left(\cos \left[(2n-1) \frac{\pi}{L} x \right] e^{-\kappa(2n-1)^2 \frac{\pi^2}{L^2} t} \right) \right)}{\left(\sum_{n=1}^{\infty} \left(\frac{1}{2n-1} \sin \left[(2n-1) \frac{\pi}{L} x \right] e^{-\kappa(2n-1)^2 \frac{\pi^2}{L^2} t} \right) \right)^2} \right) \hat{i} \quad (\text{S11})$$

Here, $e^{-(x-L/2)/L}$ ($e^{-(L/2-x)/L}$) for $L/2 \leq x \leq L$ ($0 \leq x \leq L/2$) and the plus (minus) sign in the second term on the second member is for $L/2 \leq x \leq L$ ($0 \leq x \leq L/2$). The trend of $\mathbf{F}_k^{(2)}$ is very similar for the different chemical species with a strong variation throughout the cell especially for small time.

In our 1D model, also the diffusion of molecules inside the cell occurs symmetrically along the x direction (x and $-x$ flow), namely $\mathbf{J}_{Dk} = (J_{Dk}, 0, 0)$ where $J_{Dk} = \frac{dX_{Dk}}{dt}$ with dX_{Dk} the diffusion flow of molecules. J_{Dk} is the mass diffusion flow for the k th chemical species per unit time crossing a surface of area $A = L^2$ perpendicular to the diffusion direction. It is proportional to the spatial derivative of $n_m(x, t)$, the number of moles of chemical species per unit volume (moles/m³), where $n_m(x, t)$ is generically expressed as a concentration, namely as $n_m(x, t) = N_m(x, t) / V$ with N_m the number of moles and V the volume of the solution. The diffusion equation written in the 1D case and under the assumption of uniform diffusion takes the form:

$$\frac{\partial n_{mk}(x, t)}{\partial t} = D_k \frac{\partial^2 n_{mk}(x, t)}{\partial x^2} \quad (\text{S12})$$

Here, D_k is the diffusion coefficient (m²/s) of the k th chemical species. Under the initial and boundary conditions applied to chemical species

$$\begin{cases} n_{mk}(x, 0) = \delta(x) & \text{initial condition} \\ n_{mk}(x \rightarrow \infty, t) = 0 \text{ for } t > 0 & \text{boundary condition} \end{cases} \quad (\text{S13})$$

we get the most simple solution to Equation (S12) in the form of a Gaussian distribution function

$$n_{mk}(x,t) = \frac{N_{mk}}{A} \frac{1}{\sqrt{4\pi D_k t}} e^{-\frac{\left(x-\frac{L}{2}\right)^2}{4D_k t}} \quad (\text{S14})$$

According to the initial condition in Equation (S13), it is reasonably assumed that a pulse of solute at $t = 0$ is present at a given point x that in our special case corresponds to the center of the cell $x = L/2$. In the special case, the solutes are the molecules that take part either in the cell respiration or in the lactic acid fermentation process. The boundary condition $n(x \rightarrow \infty, t) = 0$ is realistically satisfied for a value of x close to the cell membrane.

The mass diffusion flow J_{Dk} per unit time of the k th molecule (number of moles N_{mk} of the molecule per unit time crossing the surface of area A perpendicular to the flow) expressed in moles/(m² s) takes the form $J_{Dk}(x,t) = -D_k \frac{\partial n_{mk}(x,t)}{\partial x}$. The minus sign only indicates that diffusion is from the region at higher concentration to that at lower concentration. Unlike the heat flow, the mass diffusion flow has a dependence on the chemical species considered. Explicitly, by performing the spatial derivative of Equation (S14), we get:

$$\mathbf{J}_{Dk}(x,t) = \pm \frac{N_{mk}}{A} \frac{1}{4\sqrt{\pi D_k t}} \frac{(x-L/2)}{t^{3/2}} e^{-\frac{\left(x-\frac{L}{2}\right)^2}{4D_k t}} \hat{i} \quad (\text{S15})$$

Here, the plus (minus) sign is referred to the diffusion flow either along $+x$ ($L/2 \leq x \leq L$) or along $-x$ ($0 \leq x \leq L/2$) being the flow bidirectional.

In Fig. S4, we draw the diffusion flow expressed in equation (S15) for the reagents of the respiration process, viz. one mole of glucose ($N_{m \text{C}_6\text{H}_{12}\text{O}_6} = 1$) and six moles of oxygen ($N_{m \text{O}_2} = 6$) in both a normal and a cancer cell. We have carried out the calculations taking the diffusion coefficients from Tab.1 of the main text. For both chemical species the flow is of comparable magnitude, exhibits a peak close to the centre of the cell, with a broader distribution close to the centre in a normal cell especially in the first instants of time, and then a decrease going towards the border and with increasing time.

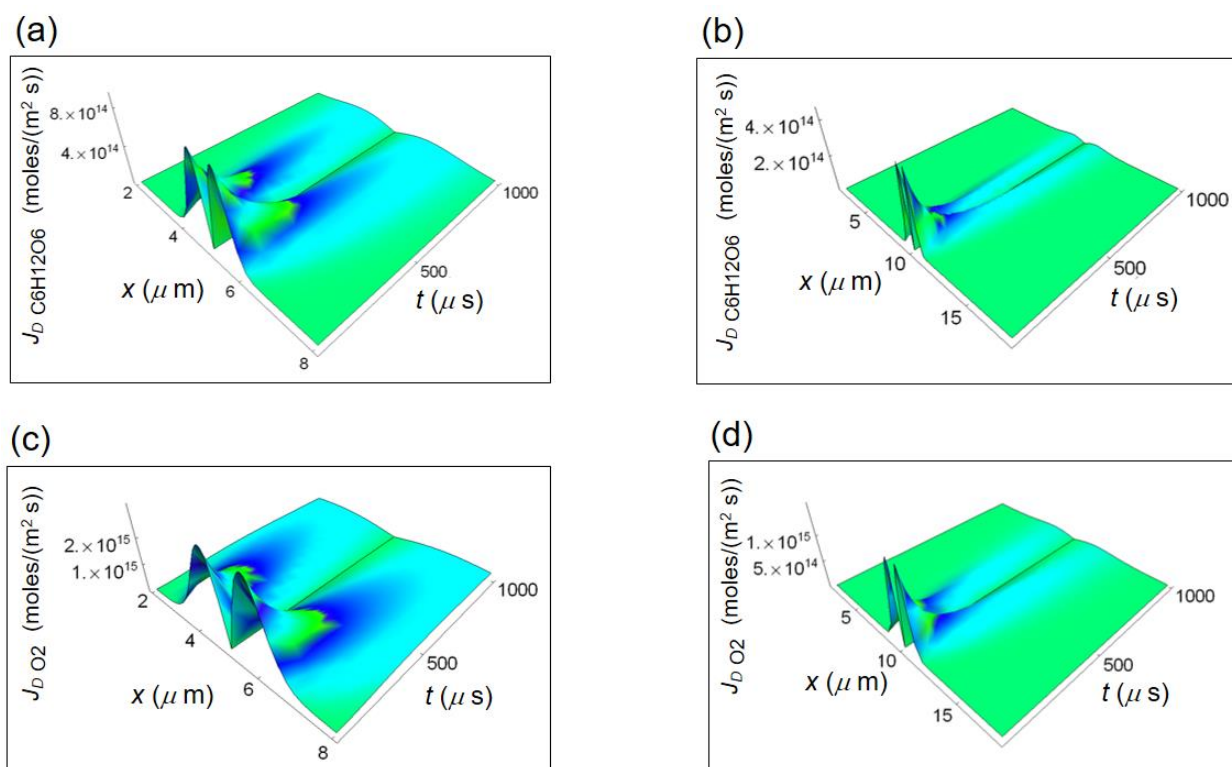


Figure S4. Diffusion flow of the reagents involved in the glucose catabolism according to equation (S15). (a) Diffusion flow of one mole of glucose molecule in a normal cell. (b) Diffusion flow of one mole of glucose molecule in a cancer cell. (c) Diffusion flow of six moles of oxygen molecule in a normal cell. (d) Diffusion flow of six moles of oxygen in a cancer cell.

In Fig. S5, we show the diffusion flow of the products of the respiration process in a normal and in a cancer cell. The behaviour is very similar to that of the reagents.

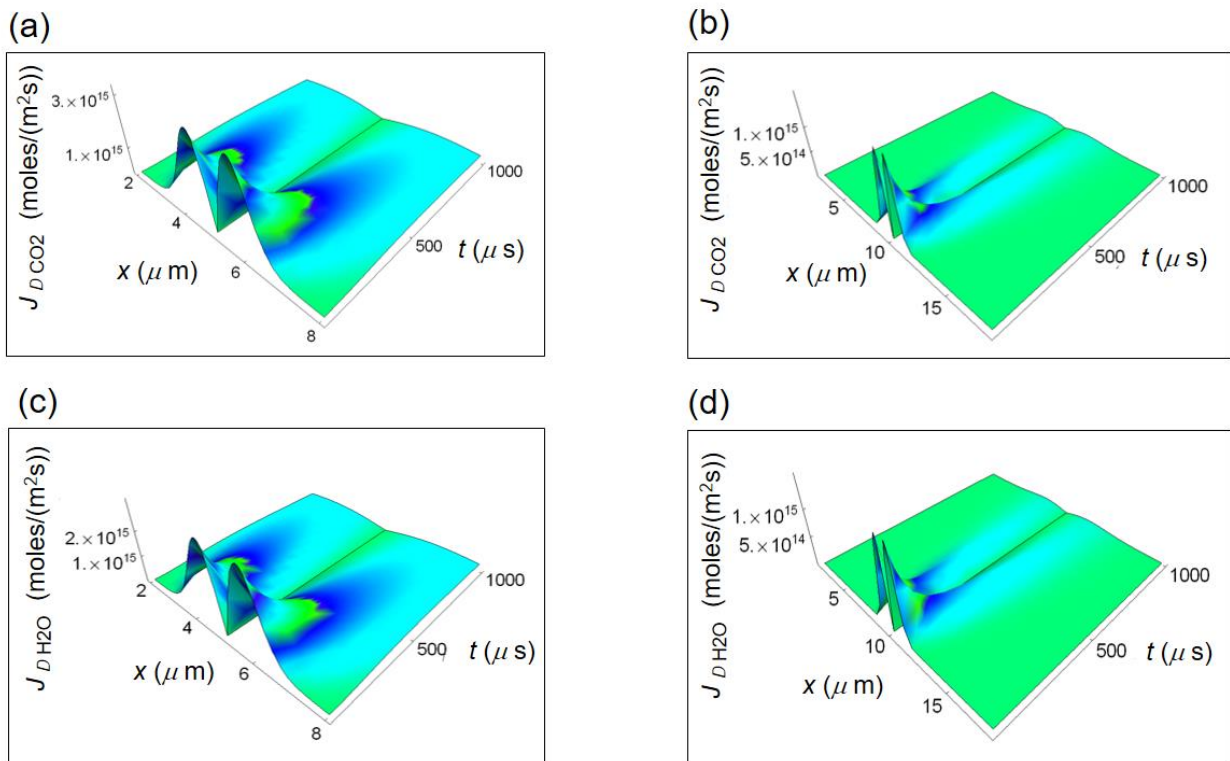


Figure S5. Diffusion flow of the products of the respiration in a cell according to equation (S15). (a) Diffusion flow of six moles of carbon dioxide molecule in a normal cell. (b) Diffusion flow of six moles of carbon dioxide molecule in a cancer cell. (c) Diffusion flow of six moles of water in a normal cell. (d) Diffusion flow of six moles of water in a cancer cell.

Fig. S6 displays the diffusion of the products of the lactic acid fermentation. Because of the large value of the diffusion constant, the diffusion flow of the hydrogen ions is significant throughout the cell during the first instants of times. Also for these chemical species, there is a decrease of the diffusion flow with increasing time.

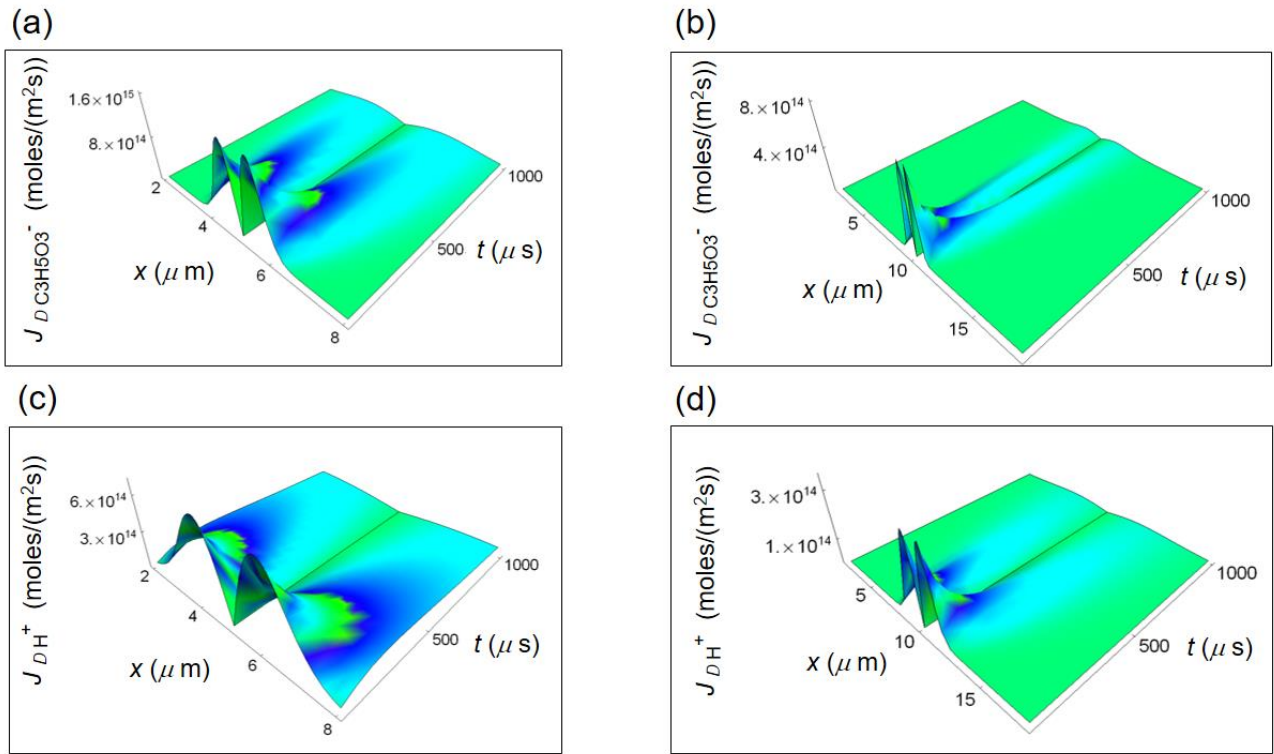


Figure S6. Diffusion flow of the products of the lactic fermentation process according to equation (S15). (a) Diffusion flow of two moles of lactate ions in a normal cell. (b) Diffusion flow of two moles of lactate ions in a cancer cell. (c) Diffusion flow of two moles of hydrogen ions in a normal cell. (d) Diffusion flow of two moles of hydrogen ions in a cancer cell.

By means of equations (S11) and (S15), we get the general expression of $r_{iD}(x,t)$ valid for any irreversible processes, viz.

$$r_{iD}(x,t) = \frac{\pi^{\frac{3}{2}}}{16} \frac{1}{T_0} \frac{1}{V_{\text{cell}}} \frac{(x-L/2)e^{-\frac{t}{\tau}}}{t^{\frac{3}{2}}} \times \sum_{k=1}^N \left(u_k \frac{N_{mk}}{\sqrt{D_k}} e^{-\frac{(x-L/2)^2}{4D_k t}} \right) \frac{\left(\sum_{n=1}^{\infty} \left(\cos \left[(2n-1) \frac{\pi}{L} x \right] e^{-\kappa(2n-1)^2 \frac{\pi^2}{L^2} t} \right) e^{-|x-L/2|/L} \right)}{\left(\sum_{n=1}^{\infty} \left(\frac{1}{2n-1} \sin \left[(2n-1) \frac{\pi}{L} x \right] e^{-\kappa(2n-1)^2 \frac{\pi^2}{L^2} t} \right) \right)^2} \quad (\text{S16})$$

after having neglected the term proportional to the sine series at the numerator that is much smaller than the one proportional to the cosine series. Equation (S16) is equation (2) of the main text.

In particular, equation (S16) applied to glucose catabolism in normal and cancer cells reads

$$r_{iD}(x,t) = \frac{\pi^{\frac{3}{2}}}{16} \frac{1}{T_0} \frac{1}{V_{\text{cell}}} \frac{(x-L/2)e^{-\frac{t}{\tau}}}{t^{\frac{3}{2}}} \times \left(w_{\text{resp}} \sum_{k=1}^{N_{\text{resp}}} \left(u_k \frac{N_{mk}}{\sqrt{D_k}} e^{-\frac{(x-L/2)^2}{4D_k t}} \right) + w_{\text{ferm}} \sum_{k=1}^{N_{\text{ferm}}} \left(u_k \frac{N_{mk}}{\sqrt{D_k}} e^{-\frac{(x-L/2)^2}{4D_k t}} \right) \right) \frac{\left(\sum_{n=1}^{\infty} \left(\cos \left[(2n-1) \frac{\pi}{L} x \right] e^{-\kappa(2n-1)^2 \frac{\pi^2}{L^2} t} \right) e^{-|x-L/2|/L} \right)}{\left(\sum_{n=1}^{\infty} \left(\frac{1}{2n-1} \sin \left[(2n-1) \frac{\pi}{L} x \right] e^{-\kappa(2n-1)^2 \frac{\pi^2}{L^2} t} \right) \right)^2} \quad (\text{S17})$$

with w_{resp} and w_{ferm} the probability weights associated to respiration and fermentation processes, respectively with $w_{\text{ferm}} = 1 - w_{\text{resp}}$ and N_{resp} and N_{ferm} the corresponding numbers of chemical species and $r_{iD}(x,t) \geq 0$.

C. RATE OF ENTROPY DENSITY PRODUCTION DUE TO IRREVERSIBLE CHEMICAL REACTIONS

We now study the term contributing to the RIEDP due to the irreversible chemical reactions. From Equation (S1) this contribution takes the general form:

$$r_{ir}(\mathbf{x},t) = \frac{1}{T(\mathbf{x},t)} \sum_{j=1}^M A_j(\mathbf{x},t) \nu_j \quad (\text{S18})$$

Here, the subscript “r” stands for reactions, the affinity of the j th reaction reads

$$A_j(\mathbf{x},t) = - \sum_{k=1}^N \nu_{kj} \mu_k(\mathbf{x},t) \quad \text{with } \nu_{kj} \text{ the stoichiometric coefficients, } N \text{ is the number of chemical}$$

species, $\mu_k(\mathbf{x}, t)$ is the space and time dependent chemical potential and $v_j = \frac{1}{V_{\text{cell}}} \frac{d\xi_j}{dt}$ is the velocity of the j th reaction, viz. the derivative of the j th degree of advancement $d\xi_j$ with respect to time divided by V_{cell} . In this framework, the affinity plays the role of the thermodynamic force and the velocity that of the corresponding thermodynamic flow associated to irreversible reactions.

In our analysis, we set $M = 1$ for every chemical reaction and we assume that flows of molecules are along the x direction so that

$$r_{i,r}(x, t) = \frac{1}{T(x, t)} A(x, t) v_1 \quad (\text{S19})$$

The affinity of every irreversible reactions taking place in the cell cytoplasm takes the form

$$A(x, t) = - \sum_{k=1}^N v_k u_k e^{-(|x-L/2|/L + t/\tau)} \quad (\text{S20})$$

and is expressed in J/moles. Instead, the corresponding velocity is $v = \frac{1}{V_{\text{cell}}} \frac{d\xi}{dt} > 0$ with $d\xi$ the variation of the degree of advance of the reaction and is in moles/ (m³ s). Irreversible chemical reactions occurring in cells are either second-order or first order. The most general expression of the velocity (rate) for a second-order reaction of the form $l A + m B \rightarrow f C$ with l , m and f the number of moles of A, B and C, respectively is

$$v = k_{\text{kin}} n_A n_B \quad (\text{S21})$$

where, $k_{\text{kin}} = K e^{-\frac{E_a}{RT_0}} > 0$ is the kinetic constant (subscript “kin” stands for kinetic) of the velocity of the reaction expressed in 1/(M s) where M is the molarity, E_a the activation energy and $R = 8.314472$ J/(mole K) the gas constant with K the pre-exponential factor and $n_A = N_{m A}/V$ ($n_B = N_{m B}/V$) is the molar concentration of reagents A (B) with $N_{m A}$ ($N_{m B}$) the number of moles of A (B). The velocity depends on the molar concentration of the two chemical species expressed by the reagent A and B. If $B = 0$ ($A = 0$) the velocity of a second-order reaction reduces to $v = k_{\text{kin}} n_A^2$ ($v = k_{\text{kin}} n_B^2$). Instead, in a first-order reaction velocity depends only on the molar concentration of a reagent

$$v = k_{\text{kin}} n_A \quad (\text{S22})$$

with k_{kin} expressed in 1/s.

Combining equations (S19), (S20) and the expression of the velocity of a reaction (equation (S21) and (S22)), we write down the RIEDP due to irreversible chemical reactions

$$r_{i r}(x, t) = -\frac{\pi}{4} \frac{1}{T_0} \frac{1}{V_{\text{cell}}^{p+q}} \frac{k_{\text{kin}} \sum_{k=1}^N v_k u_k e^{-(x-L/2)/L+t/\tau} N_{m \text{ A reag}}^p N_{m \text{ B reag}}^q}{\sum_{n=1}^{\infty} \left(\frac{\sin \left[(2n-1) \frac{\pi}{L} \left(\frac{L}{2} - x \right) \right]}{2n-1} e^{-\kappa(2n-1)^2 \frac{\pi^2}{L^2} t} \right)} \quad (\text{S23})$$

Here $p=0, 1, 2$, $q=0, 1, 2$ and $p+q=1, 2$ for first- and second-order irreversible chemical reactions, respectively and $N_{m \text{ A reag}}/V_{\text{cell}}$ ($N_{m \text{ B reag}}/V_{\text{cell}}$) is the molar concentration of reagents A and B, respectively taking the volume of the solution equal to V_{cell} .

We now apply this formalism to glucose catabolism given by a sequence of reactions of glucose catabolism, either as respiration or as lactic acid fermentation process, classified as first-order. For

this special case, we write $v = \frac{1}{V_{\text{cell}}} \frac{dN_{m \text{ C}_6\text{H}_{12}\text{O}_6}}{dt} / v_{\text{C}_6\text{H}_{12}\text{O}_6} = -\frac{dn_{\text{C}_6\text{H}_{12}\text{O}_6}}{dt} > 0$ being $dN_{m \text{ C}_6\text{H}_{12}\text{O}_6} / v_{\text{C}_6\text{H}_{12}\text{O}_6} = d\xi$

with $v_{\text{C}_6\text{H}_{12}\text{O}_6} = -1$ the glucose stoichiometric coefficient and $dn_{\text{C}_6\text{H}_{12}\text{O}_6} = \frac{1}{V_{\text{cell}}} dN_{m \text{ C}_6\text{H}_{12}\text{O}_6} < 0$ the

variation of glucose molarity (variation of the concentration of glucose moles in the solution of volume equal to V_{cell}) with $N_{m \text{ C}_6\text{H}_{12}\text{O}_6}$ the number of moles of glucose (alternatively, one could choose

$-\frac{1}{6} \frac{dn_{\text{O}_2}}{dt}$ with n_{O_2} the molar concentration of the oxygen, the second reagent of the glycolytic

process). In the special case, $N_{m \text{ C}_6\text{H}_{12}\text{O}_6} = 1$ and $dN_{m \text{ C}_6\text{H}_{12}\text{O}_6} = -1$ in all studied reactions.

Specifically, $N_{m \text{ C}_6\text{H}_{12}\text{O}_6} = N^{\text{C}_6\text{H}_{12}\text{O}_6} / N_A$ where $N^{\text{C}_6\text{H}_{12}\text{O}_6}$ is number of glucose molecules and $N_A = 6.02 \times 10^{23}$ is the Avogadro number. Explicitly, the affinity of glucose catabolism reads

$$A(x, t) = -\left(w_{\text{resp}} \sum_{k=1}^{N_{\text{resp}}} v_k u_k e^{-(x-L/2)/L+t/\tau} + w_{\text{ferm}} \sum_{k=1}^{N_{\text{ferm}}} v_k u_k e^{-(x-L/2)/L+t/\tau} \right) \quad (\text{S24})$$

Here, w_{resp} and w_{ferm} are the probability weights associated to respiration and fermentation processes, respectively with $w_{\text{ferm}} = 1-w_{\text{resp}}$ and N_{resp} and N_{ferm} are the corresponding numbers of chemical species.

In Fig. S7, we plot the affinity for a normal cell (panel (a)) and for a cancer cell (panel (b)). In the numerical calculations, we have taken the following parameters: $w_{\text{resp}} = 0.8$ (0.1) and $w_{\text{ferm}} = 0.2$ (0.9) for a normal (cancer) cell⁵, $\tau = 10^{-4}$ s, $k_{\text{kin}} = 10^{-4}$ /s for normal cells and $k_{\text{kin}} = 10^{-5}$ /s for cancer cells [S6]. The values used for the chemical potentials at $x = L/2$ and $t = 0$ (partial molar energy) of the different chemical species are the ones in Table 1 of the main text.

In both cases, the affinity tends to zero with increasing time as should be expected for every thermodynamic system moving towards equilibrium. Looking at Fig. S7, it turns out that the affinity for a normal cell is one order of magnitude greater than the corresponding one for a cancer cell. This means that the thermodynamic force associated to the glucose catabolism reaction in a cancer cell is weaker with respect to that of the corresponding normal cell.

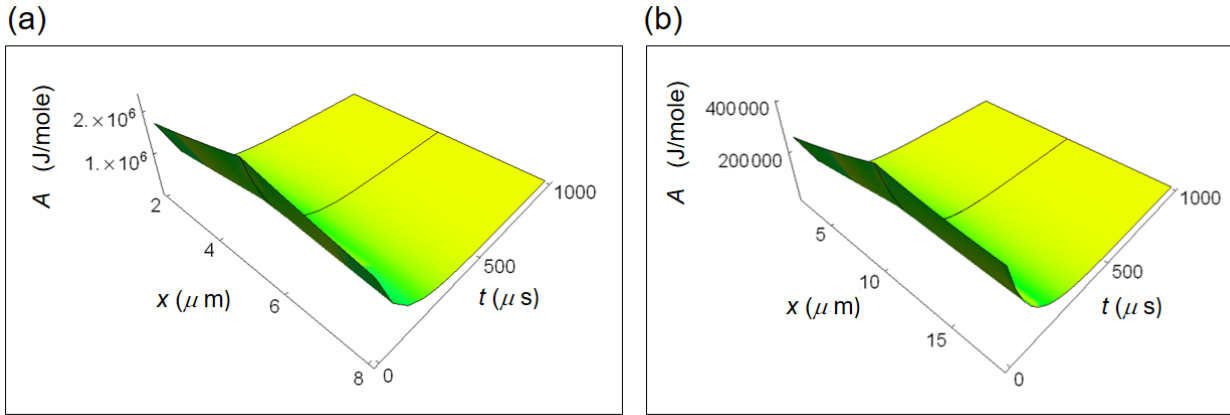


Figure S7. Affinity for a cell calculated by means of equation (S24). (a) Affinity for a normal cell. (b) Affinity for a cancer cell.

Like for other first-order reactions, we write the velocity of the glucose catabolism in the form

$$v = k_{\text{kin}}^{\text{resp (ferm)}} n_{C_6H_{12}O_6} \quad (\text{S25})$$

with $k_{\text{kin}}^{\text{resp (ferm)}} > 0$ the pathway “kinetic constant” of the respiration (fermentation) process expressed in 1/s.

For the case of glucose catabolism that can be regarded as a first-order reaction, equation (S23) becomes

$$r_{i_r}(x,t) = -\frac{\pi}{4} \frac{1}{T_0} \frac{1}{V_{\text{cell}}} \times \frac{k_{\text{kin}} \left(w_{\text{resp}} \sum_{k=1}^{N_{\text{resp}}} v_k u_k e^{-\left(\frac{|x-L/2|}{L+t/\tau}\right)} N_{m \text{ C}_6\text{H}_{12}\text{O}_6} + w_{\text{ferm}} \sum_{k=1}^{N_{\text{ferm}}} v_k u_k e^{-\left(\frac{|x-L/2|}{L+t/\tau}\right)} N_{m \text{ C}_6\text{H}_{12}\text{O}_6} \right)}{\sum_{n=1}^{\infty} \left(\frac{\sin \left[(2n-1) \frac{\pi}{L} \left(\frac{L}{2} - x \right) \right]}{2n-1} e^{-\kappa(2n-1)^2 \frac{\pi^2}{L^2} t} \right)} \quad (\text{S26})$$

by taking into account the mixed nature of glucose catabolism occurring in both types of cells (both respiration and fermentation process). Here, $e^{-\frac{(L/2-x)}{L}}$ for $0 \leq x \leq L/2$ and $e^{-\frac{(x-L/2)}{L}}$ for $L/2 \leq x \leq L$ and $r_{i_r}(x,t) \geq 0$. The subscript r stands for “irreversible reactions”. Equation (S26) is equation (3) of the main text.

For both normal and cancer cell, it is always $\lim_{t \rightarrow \infty} r_{i_r}(x,t) = 0$, namely each contribution to the RIEDP vanishes when the thermodynamic system reaches the global equilibrium.

3. RATE OF EXTERNAL ENTROPY DENSITY PRODUCTION

The human cell (either normal or cancer cell) behaves like an open thermodynamic system. This means that it exchanges energy and matter with the intercellular environment. In this respect, it is useful to define the rate $r_e(\mathbf{x},t)$ of external entropy density production (REEDP) giving the amount of local entropy density outside a cell in the intercellular environment. Specifically, the REEDP has a contribution related to heat diffusion linked to energy exchange between the cell and the intercellular environment and a contribution due to matter exchange with the intercellular environment in terms of variation of the number of moles. No terms related to diffusion flow are present. Like for the calculation of the RIEDP due to heat flow, for the calculation of the REEDP we reasonably suppose that the temperature of the intercellular environment is spatially non-uniform and has a time dependence seeking for a solution to the heat equation free from boundary conditions.

Strictly speaking, for a thermodynamic system the infinitesimal entropy density exchanged between the cell and the environment due to heat release is $ds_e Q = \frac{1}{V_{\text{cell}}} \frac{dQ}{T_{\text{ic}}(x,t)}$, where $dQ = dU + p dV$ is the infinitesimal heat transfer with U the internal energy, p the pressure and $T_{\text{ic}}(x,t)$ the space and time dependent intercellular temperature distribution where the subscript “ic” stands for intercellular. Therefore, the external contribution to the infinitesimal entropy density consists of two terms, viz. $ds_e = ds_{eQ} + ds_{e,r}$ with $ds_{e,r}$ the mass contribution associated to irreversible exchanges of molecules with the intercellular environment.

In our 1D model, we express the REEDP as $r_e(x,t) = r_{eQ}(x,t) + r_{e\text{exch}}(x,t)$ where $r_{eQ}(x,t)$ is the REEDP associated to heat flow, while $r_{e\text{exch}}(x,t)$ is due to exchanges of matter of the cell with the intercellular environment where the subscript “exch” stands for exchange. This scheme is valid for both a normal and a cancer cell.

Explicitly

$$r_e(x,t) = \frac{1}{T_{\text{ic}}(x,t)} \left(\frac{du(x,t)}{dt} + \frac{1}{V_{\text{cell}}} p(x,t) \frac{dV}{dt} \right) - \frac{1}{T_{\text{ic}}(x,t)} \sum_{k=1}^{N_{\text{pr}}} \mu_k(x,t) \frac{d_e N_{m,k}}{dt} \quad (\text{S27})$$

Here, $u = U/V_{\text{cell}}$ is the internal energy density. The second term on the second member expresses the matter flow with the external environment being $d_e N_{m,k}$ the variation of the number of moles of the products of the catabolic reaction and N_{pr} is the number of chemical species of products. By neglecting the small cell volume variation occurring during the entropy transfer ($dV/dt \approx 0$) we get

$$r_e(x,t) \approx \frac{1}{T_{\text{ic}}(x,t)} \left(\frac{du(x,t)}{dt} - \sum_{k=1}^{N_{\text{pr}}} \mu_k(x,t) \frac{d_e N_{m,k}}{dt} \right) \quad (\text{S28})$$

A. RATE OF EXTERNAL ENTROPY DENSITY PRODUCTION ASSOCIATED TO HEAT FLOW

In an open thermodynamic system like the human cell (either normal or cancer), part of the entropy exchanged with the extracellular environment is proportional to the variation of produced heat

according to the entropy definition in a thermodynamic system and cannot be calculated according to the internal heat flow valid for determining the RIEDP.

Keeping in mind that water is the main component of a human cell, from a thermodynamic point of view a cell (either normal or cancer cell) can be described as a fluid. Moreover, irreversible chemical reactions occur in a vapor phase where vapor is a substance that is a mixture between a gaseous and a liquid phase at room temperature. Hence, without loss of generality, we describe heat exchange with the environment in a way similar to heat exchange for an ideal gas. Owing to this thermodynamic analogy, the cell energy is thus equivalent to the gas kinetic energy. Hence, in the thermodynamic limit, namely ideally assuming that the volume increases with the number of molecules that in a cell is very high, the cell energy has a continuous spectrum of values. Its derivation, in the simplest picture, starts from the partition function of a monoatomic gas. Note that water in the gaseous phase behaves not like a monoatomic gas but like a triatomic gas. However, without loss of generality, the kinetic energy due to the rotation and vibration of water molecules typical of polyatomic molecules is much smaller than the translational kinetic energy that is instead associated to heat flow and this justifies the analogy with a monoatomic gas where only translational degrees of freedom are present. Moreover, within this description we do not take into account also the potential energy due to intermolecular forces among water molecules that does not play a role in heat flow. Straightforwardly, the partition function Z of an ideal monoatomic gas, that is equivalent within this description to the cell partition function, is expressed by the well-known formula $Z = A T^{\frac{3}{2}}$ where $A = V_{\text{cell}} (2 k_B m)^{3/2} / h^3$ with $k_B = 1.3805 \times 10^{-23}$ J/K the Boltzmann constant, m the mass and h the Planck constant [S7]. From the well-known relation between the average energy and the partition function, viz. $\bar{E} = k_B T^2 \frac{d}{dT} \ln Z$ we get $U(x, t) = 3/2 N k_B T(x, t)$, where the internal energy is a thermal energy and has a space and time dependence getting its largest contribution from kinetic energy. Here, $U = N \bar{E}$ being N the number of molecules carrying the kinetic energy (translational and vibrational) and $N = N_m N_A$ where N_m is the number of moles of the products of glucose catabolism (respiration process for the normal cell and lactic fermentation for the cancer cell) and $N_A = 6.02 \times 10^{23}$ molecules is the Avogadro number. As expected, the internal energy of the cell due to heat exchange with the intercellular environment turns out to be proportional to T and depends on time t via the temperature.

We write down the well-known fundamental solution to the heat equation (equation (S3)) obtained with no boundary conditions since we are considering the intercellular environment and we are

making some consideration about the finite heat quantity flowing towards the intercellular environment, viz.

$$T_{ic}(x, t) = \frac{T_{ic} x_0}{\sqrt{4\pi\kappa t}} e^{-\frac{(x-L)^2}{4\kappa t}} \quad (\text{S29})$$

Here, $x > L$, T_{ic} is the maximum intercellular temperature and x_0 is a characteristic length in the intercellular environment over which the temperature varies. In the model calculations, we have taken the realistic value $x_0 = 10$ nm such that the temperature in the intercellular space at the border with the cell and especially at the initial instant of times when the release of heat takes place is about 310 K. We show the temperature distribution in the intercellular environment of both a normal and a cancer cell in Fig. S8.

Although in some cancer tissues the separation between adjacent cells vanishes because of the tumor, we have taken the value of the separation of about 0.2-0.3 μm between two adjacent normal cells and about 1.5 μm between two cancer cells considering the typical values for the epithelial cells of human breast tissue [S8]. There is a maximum temperature close to the border between the cell and the intercellular environment and T_{ic} tends to decrease slightly by going away from the cell. Of course, for a realistic description we should take into account also the temperature distribution of the adjacent cell (not shown) but it would be outside the aims of this approach that focuses on the thermodynamic behaviour of a single cell.

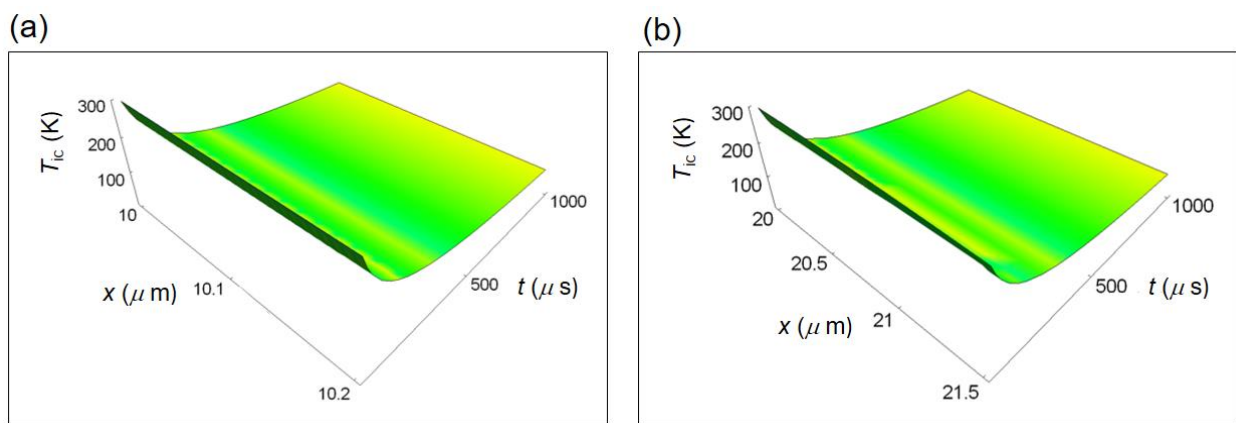


Figure S8. Intercellular temperature distribution calculated according to equation (S3) and expressed in equation (S29). (a) Temperature distribution in the intercellular environment for a normal cell. (b) Temperature distribution in the intercellular environment for a cancer cell.

The time derivative, calculated via the expression $U(x, t) = 3/2 N k_B T_{ic}(x, t)$, reads approximately

$$\frac{d u(x, t)}{dt} \approx \frac{1}{V_{\text{cell}}} \frac{3}{2} k_B N \frac{T_{ic}(x, t) (\kappa(x-L)^2) \sqrt{4\pi\kappa t}}{8(\kappa t)^2 \sqrt{\pi\kappa t}}$$

taking into account that, for x large and small t , $\kappa(x-L)^2 \gg \kappa^2 t$. The REEDP related to heat transport from the cell to the intercellular environment is approximately

$$r_{eQ}(x, t) \approx \frac{1}{T_{ic}(x, t)} \frac{d u(x, t)}{dt} \quad (\text{S30})$$

We substitute $\frac{d u(x, t)}{dt}$ getting

$$r_{eQ}(x, t) \approx \frac{1}{V_{\text{cell}}} \frac{3}{8} k_B \frac{N_A N_{m \text{ pr}}}{\kappa} \frac{(x-L)^2}{t^2} \quad (\text{S31})$$

where, $N_{m \text{ pr}}$ are the number of moles of the products for the studied irreversible chemical reaction.

Equation (S31) is general and valid for describing r_{eQ} associated to external heat transport due to irreversible processes in normal and cancer cells. Equation (S31) is equation (4) of the main text. If applied to glucose catabolism we need to take into account the weights associated to respiration and fermentation processes yielding

$$r_{eQ}(x, t) \approx \frac{1}{V_{\text{cell}}} \frac{3}{8} k_B \frac{N_A (N_{m \text{ pr resp}} w_{\text{resp}} + N_{m \text{ pr ferm}} w_{\text{ferm}})}{\kappa} \frac{(x-L)^2}{t^2} \quad (\text{S32})$$

$N_{m \text{ pr resp}} (N_{m \text{ pr ferm}})$ is the number of moles of the products in respiration (fermentation) process.

B. IRREVERSIBLE EXCHANGES WITH THE INTERCELLULAR ENVIRONMENT

The REEDP due to mass transport related to irreversible exchanges with the intercellular environment for any irreversible reaction occurring either in a normal or in a cancer cell is

$$r_{e \text{ exch}}(x, t) = -\frac{1}{T_{ic}(x, t)} \frac{1}{V_{\text{cell}}} \sum_{k=1}^{N_{\text{pr}}} \mu_k(x, t) \frac{d_e N_{m k}}{dt} \quad (\text{S33})$$

where $d_e N_{m k}$ is the variation of the number of moles of the k th product of the irreversible reaction with the subscript “e” indicating external and N_{pr} is the number of products with “pr” labelling products.

Substituting the expressions of the intercellular temperature distribution $T_{ic}(x, t)$ given in equation (S29), of the chemical potential $\mu_k(x, t) = u_k e^{-(|x-L|/2L + t/\tau)}$ and inserting the time $d\tau_1$ that is a characteristic time of the order of the inverse of k_{kin} , we get

$$r_{e \text{ exch}}(x, t) = -\frac{1}{T_{ic}} \frac{1}{V_{\text{cell}}} \frac{\sqrt{4\pi\kappa}}{x_0} t^{\frac{1}{2}} e^{\frac{(x-L)^2}{4\kappa t}} \sum_{k=1}^{N_{\text{pr}}} u_k e^{-(|x-L|/2L + t/\tau)} \frac{d_e N_{m k}}{d\tau_1} \quad (\text{S34})$$

Equation (S34) is equation (5) of the main text.

In particular, for glucose catabolism $r_{e \text{ exch}}$ takes the general form

$$r_{e \text{ exch}}(x, t) = -\frac{1}{T_{ic}(x, t)} \frac{1}{V_{\text{cell}}} \left(w_{\text{resp}} \sum_{k=1}^{N_{\text{pr resp}}} \mu_k(x, t) \frac{d_e N_{m k \text{ resp}}}{dt} + w_{\text{ferm}} \sum_{k=1}^{N_{\text{pr ferm}}} \mu_k(x, t) \frac{d_e N_{m k \text{ ferm}}}{dt} \right) \quad (\text{S35})$$

Here, $N_{\text{pr resp}}$ ($N_{\text{pr ferm}}$) is the number of products of respiration (fermentation) and $d_e N_{m k \text{ resp}}$ ($d_e N_{m k \text{ ferm}}$) is the variation of the number of moles moles of the products in the respiration (fermentation) process.

Substituting the expressions of $T_{ic}(x, t)$ expressed in equation (S29) and of the chemical potential we get

$$r_{e \text{ exch}}(x, t) = -\frac{1}{T_0} \frac{1}{V_{\text{cell}}} \frac{\sqrt{4\pi\kappa t}}{x_0} e^{\frac{(x-L)^2}{4\kappa t}} \times \left(w_{\text{resp}} \sum_{k=1}^{N_{\text{pr resp}}} u_k e^{-(|x-L|/2L + t/\tau)} \frac{d_e N_{m k \text{ resp}}}{d\tau_1} + w_{\text{ferm}} \sum_{k=1}^{N_{\text{pr ferm}}} u_k e^{-(|x-L|/2L + t/\tau)} \frac{d_e N_{m k \text{ ferm}}}{d\tau_2} \right) \quad (\text{S36})$$

where, $d\tau_1$ ($d\tau_2$) is a characteristic time such that $1/d\tau_1$ ($1/d\tau_2$) is about $10^{-5}/\text{s}$ ($10^{-4}/\text{s}$), namely of the order of the pathway kinetic constant of the glucose catabolism reaction in both processes.

By analysing the behaviour of the three contributions to REEDP it is $\lim_{t \rightarrow \infty} r_e(x,t) = 0$. Hence, we have proved that the equilibrium state of an open thermodynamic system like a cell (either normal or cancer), where irreversible processes take place, implies the minimization of both r_i and r_e with increasing time and its vanishing in the limit of infinite time.

References

- S1. Kondepudi, D. & Prigogine, I. *Modern thermodynamics: From heat engines to dissipative structures* (Wiley, 2015).
- S2. Dolfi, C.S. *et al.* The metabolic demands of cancer cells are coupled to their size and protein synthesis rate. *Cancer & Metabol.* **1**, 1-13 (2013).
- S3. Apps, D.K. & Nairn, A.C. The equilibrium constant and the reversibility of the reaction catalysed by nicotinamide-adenine dinucleotide kinase from pigeon liver. *Biochem. J.* **167**, 87-93 (1977).
- S4. Pessôa, C. A., Gushikem, Y. & Kubota, T. K. Ferrocenecarboxylic acid adsorbed on Nb₂O₅ film grafted on a SiO₂ surface: NADH oxidation study. *Electrochim. Acta* **46**, 2499-2505 (2001).
- S5. Warburg, O. On respiratory impairment in cancer cells. *Science* **124**, 269–270 (1956).
- S6. Beck, W.S. A kinetic analysis of the glycolytic rate and certain glycolytic enzymes in normal and leukemic leucocytes. *J. Biol. Chem.* **216**, 333-350 (1955).
- S7. Alonso, M. & Finn, E.J. *Quantum and statistical physics Vol. 3* (Addison Wesley, 1968).
- S8. Ozzello, L. Ultrastructure of human mammary carcinoma cells in vivo and in vitro. *J. Natl. Cancer Inst.* **48**, 1043-1050 (1972).